Université du Québec
Institut national de la recherche scientifique
Centre Eau Terre Environnement

ÉTUDE EN LABORATOIRE DE L'INJECTION DE MOUSSE POUR LE TRAITEMENT DE SOLS CONTAMINÉS AUX HYDROCARBURES

Par

Mélanie Longpré-Girard

Mémoire présenté pour l'obtention du grade de
Maître ès sciences (M.Sc.)
en Sciences de la Terre

Jury d'évaluation

Président du jury et examinateur interne	Guy Mercier INRS ETE
Examinateur externe	Daniel Cassidy Western Michigan University
Directeur de recherche	Richard Martel INRS ETE
Codirecteur de recherche	René Lefebvre INRS ETE

REMERCIEMENTS

Je tiens tout particulièrement à remercier Thomas Robert pour l'aide et les encouragements qu'il m'a patiemment prodigués durant chacune des étapes de ce projet. Je tiens également à remercier mes directeur et codirecteur Richard Martel et René Lefebvre pour tout le support qu'ils m'ont apporté. Je tiens particulièrement à les remercier pour la liberté qu'ils m'ont accordée autant dans l'élaboration que dans l'exécution de ce projet. Je veux remercier Jean-Marc Lauzon et TechnoRem pour leur intérêt dans le projet. Je me dois aussi de remercier tous les gens merveilleux de l'équipe de l'INRS qui m'ont aidé pendant le projet : Luc Trépanier, Uta Gabriel et Richard Lévesque.

Et je remercie spécialement mes amis et ma famille qui m'ont soutenu tout au long de ce projet. Enfin, je tiens à remercier Guillaume Lefrançois, qui m'a supportée avec affection tout au long de ce projet.

RÉSUMÉ

L'injection de mousse pour la réhabilitation de sols contaminés aux hydrocarbures légers est une méthode prometteuse. Ce projet porte sur le développement d'une méthodologie de production de mousse et sur l'étude du comportement rhéologique de cette mousse lorsqu'elle est injectée dans un milieu poreux hétérogène. Plusieurs solutions tensioactives ont été testées afin d'identifier le meilleur candidat pour le traitement de sable de silice hétérogène contaminé au p-xylène. Les tensioactifs ont été départagés suivant leur capacité à produire de la mousse via des mesures Ross Miles et leur habilité à abaisser la tension interfaciale de la solution avec le p-xylène grâce à la méthode de la goutte pendante. Pour les tensioactifs sélectionnés, il a été constaté que le test Ross Miles fournit une comparaison adéquate des propriétés moussantes des solutions puisque les candidats ayant eu les meilleurs résultats Ross Miles ont par la suite produit les mousses les plus visqueuses en colonne. D'autres essais en colonne ont indiqué que pour obtenir le front de mousse le plus stable et visqueux possible, il faut utiliser une colonne de production de mousse, pré-rincer la colonne avec la solution tensioactive avant l'injection de la mousse et utiliser une pression d'injection élevée.

Un bac 2D contenant deux couches de sables de granulométries différentes a été utilisé pour évaluer le contrôle de mobilité obtenu lors de l'injection la mousse. Le contraste de perméabilité entre les deux couches a été constaté lors de l'essai de traçage où des fronts de traceur en forme de piston ayant des vitesses différentes dans chaque couche ont été observés. L'essai d'injection de mousse dans le bac non contaminé a permis l'observation d'un front en forme de « S » avançant à la même vitesse dans chaque couche ce qui indique un meilleur contrôle de mobilité que lors de l'essai de traçage. Suite à la contamination du bac au p-xylène, un essai de traçage a permis de constater l'augmentation du contraste de perméabilité entre les deux couches de sable. Un premier traitement avec une solution tensioacive a eu pour effet de remobiliser une partie du p-xylène sans en récupérer à la sortie du bac. L'injection de mousse a permis d'atteindre une saturation résiduelle sous la limite de détection de 16 mg/kg dans les zones balayées par la mousse ce qui est sous le critère (50 mg/kg) acceptable pour un terrain à usage industriel. Une portion de la récupération du p-xylène s'est faite par mobilisation (19%) et solubilisation (16%) et une portion s'est faite par volatilisation mais n'a pas été complètement comptabilisée. Une optimisation du procédé reste à faire pour des applications futures à faible profondeur incluant la quantification de la volatilisation ainsi que la diminution des pressions requises pour la génération et l'injection de la mousse.

TABLE DES MATIÈRES

LISTE DES TABLEAUX

LISTE DES FIGURES

CHAPITRE 1 : INTRODUCTION

1.1 Cadre du projet

Cette étude a été réalisée dans l'optique d'une application de mousses produites avec des tensioactifs en solutions aqueuses sur des sites contaminés aux liquides immiscibles légers (LIL). Ce projet est financé par une subvention de recherche et développement coopérative du Conseil de Recherches en sciences naturelles et en génie du Canada (CRSNG-RDC) en partenariat avec TechnoRem, Laval, Canada. Il vise à étudier le comportement des mousses en laboratoire dans l'optique d'une application à l'échelle terrain pour réhabiliter des sites contaminés aux LIL.

1.1.1 Restauration in situ à l'aide de solutions tensioactives

L'utilisation des solutions tensioactives pour récupérer des hydrocarbures dans les sols a été extensivement étudiée par le passé. L'industrie pétrolière est responsable d'une majeure partie des recherches sur les tensioactifs menées en récupération assistée du pétrole (RAP) dans les réservoirs pétroliers profonds (Lake, 1989). Cependant, les conditions sont différentes entre les réservoirs pétroliers profonds et les sédiments contaminés peu profonds. Les réservoirs pétroliers sont souvent situés à des profondeurs où la température et les pressions d'injection des fluides sont élevées sans craintes d'instabilités ou de fracturation du réservoir. Dans les sédiments peu profonds, les températures sont basses et les fluides doivent être injectés à une pression qui n'excède pas la masse de sol saturée au-dessus de la zone traitée pour ne pas engendrer d'instabilités et un soulèvement des sols (Chowdiah et al.,1998). De plus, les solutions utilisées en traitement de sédiments doivent être biodégradables et non toxiques puisqu'une migration post-traitement est possible. En RAP, les profondeurs auxquelles les fluides sont injectés étant grandes, la migration des produits vers des récepteurs potentiels est improbable et la toxicité des tensioactifs n'est pas aussi critique qu'en environnement.

L'instabilité du front d'injection est un problème majeur relié à l'utilisation de solutions liquides pour la récupération de LI (Lake, 1989). Cette instabilité fait en sorte qu'une partie seulement des hydrocarbures contenus dans le milieu poreux hétérogène est contactée par la solution tensioactive et les hydrocarbures non contactés ne peuvent pas être récupérés. Une des solutions à ce problème est l'utilisation de fluides rhéofluidifiants tels que les polymères

combinés avec la solution tensioactive. Ces fluides stabilisent le front d'injection et assurent le passage du fluide injecté non seulement dans les couches très perméables mais aussi dans les couches de faible perméabilité qui ne seraient normalement pas contactées par les tensioactifs. Cette option a été étudiée dans le cadre de nombreuses recherches (Martel, 1995; Martel et al.,1998; Martel et al., 2004; Silva et al., 2012; Robert et al., 2006). Les polymères agissent de deux façons : ils augmentent la viscosité de la solution ce qui assure la stabilité du front du fluide injecté, et leur propriété rhéofluidifiantes entraînent une diminution de la viscosité lorsque la force de cisaillement est élevée comme c'est le cas près des puits d'injection et lors du passage dans des horizons de sédiments fins.

1.1.2 Restauration in situ à l'aide des mousses

Tout comme certains polymères, la mousse possède des propriétés nonnewtoniennes et rhéofluidifiantes (Hirasaki et Lawson, 1985; Falls et al., 1989). De plus, la présence d'air entraîne une diminution de la perméabilité relative du milieu à l'eau ce qui permet un meilleur contrôle de mobilité (Li, 2011). Le grès fracturé est souvent considéré comme un milieu poreux favorable à l'injection de mousse en RAP (Simjoo et al., 2012; Nguyen et al.. 2007). Plusieurs études ont été menées sur les mousses pour la réhabilitation de sites contaminés par des liquides immiscible denses (LID) tels que le TCE (Jeong and Corapcioglu, 2000, 2003, 2005; Rothmel et al., 1998; Pennell et al., 1996). Cependant, pour ce type de contamination, la mobilisation du contaminant n'est pas désirée puisque le contaminant plus dense que l'eau peut être entraîné en profondeur ce qui le rend plus difficile à récupérer. Dans le cas d'un LIL, la migration verticale ne pose pas problème étant donné qu'il a tendance à migrer vers le haut de la zone saturée, ce qui le rend plus facile à récupérer. Cette étude a été réalisée dans l'optique de traiter un LIL avec des mousses capables de mobiliser la contamination trappée dans un milieu poreux hétérogène peu profond.

1.2 Objectifs de recherche

L'objectif principal de cette étude est de développer une méthodologie pour la sélection d'un tensioactif et pour la production de mousse dans le but de traiter une contamination au LIL dans des sédiments peu profonds. Pour atteindre cet objectif, les objectifs secondaires suivants ont été fixés :

- Sélectionner un tensioactif capable de produire une mousse propice à la récupération de LIL trappé dans des sédiments peu profonds. Cette sélection est basée sur la caractérisation des propriétés de la mousse (qualité de la mousse, viscosité de la mousse et capacité à mousser) ainsi que sur le pouvoir mobilisant du tensioactif;
- Produire de la mousse ex situ et l'injecter dans un milieu poreux homogène afin de la caractériser sous des conditions représentatives de sédiments peu profonds ainsi que de vérifier l'effet sur le comportement de la mousse de deux conditions: la pression d'injection, le prélavage du milieu poreux avec de l'eau ou le tensioactif en solution utilisé pour produire la mousse;
- Dans un bac de sable 2D, évaluer l'effet de l'hétérogénéité sur le comportement de la mousse ainsi que la récupération de LIL grâce à son injection dans un milieu poreux constitué de deux couches de sables superposées de perméabilités différentes.

Plusieurs types de tensioactifs ont été évalués pour leur capacité à produire de la mousse et à mobiliser le contaminant. Les propriétés d'écoulement de la mousse en milieu poreux 1D sont évaluées grâce à des colonnes d'acrylique transparentes simulant un milieu poreux homogène. Les propriétés de la mousse sont observées dans ces colonnes par suivi visuel et des pressions dans le système. L'étude de l'écoulement de la mousse en milieu hétérogène est possible grâce à la conception et la production d'un bac 2D permettant de reproduire en laboratoire un milieu poreux stratifié constitué de deux couches de sable de perméabilités différentes. Des essais d'injection de traceur et de mousse ont été effectués dans le bac avant sa contamination. Des essais de traçage, de traitement avec une solution tensioactive et de traitement avec de la mousse ont été effectués dans le bac contaminé.

1.3 Organisation du mémoire

L'utilisation de mousses tensioactives pour la récupération de LIL dans des sédiments de surface nécessite la compréhension des principes théoriques reliés aux mousses ainsi qu'à l'écoulement de fluides de traitement dans les sols. Le chapitre 2 présente une courte revue de ces principes et fait état des différences entre les applications dans les domaines pétrolier et environnemental. Le chapitre 3 est présenté sous forme d'article et est consacré au choix du tensioactif et aux essais en colonne 1D. Les principaux résultats sont discutés dans l'optique de

fournir des indications pour les essais en bac 2D présentés au Chapitre 4. Ce dernier prend aussi la forme d'un article et porte sur les essais en bac de sable; la méthodologie utilisée ainsi que les résultats des différents essais effectués. Le chapitre 5 fait état des principales conclusions tirées au cours du projet

Les chapitres 3 et 4 présentent le corps du projet, plusieurs auteurs ont donc participé à leur réalisation. L'auteure du présent mémoire a effectué la planification ainsi que l'exécution des essais de laboratoire. Elle a aussi effectué la rédaction des deux articles présentés. Thomas Robert a participé à l'exécution de certains essais de laboratoire ainsi qu'à la planification de la méthodologie utilisée dans le cadre du projet. Richard Martel, René Lefebvre et Jean-Marc Lauzon ont effectué la planification du projet. Richard Martel et René Lefebvre ont effectué la révision des articles ainsi que la validation de la méthodologie utilisée. Jean-Marc Lauzon a participé au financement du projet par l'entremise de TechnoRem.

CHAPITRE 2 : THÉORIE

2.1 Introduction

Au Québec, en 2010, 65% de sites contaminés recensés par l'actuel Ministère du Développement durable de l'Environnement et de la Lutte contre les changements climatiques (MDDELCC) contenaient des hydrocarbures C_{10}-C_{50} (Hébert et Bernard, 2013). Une des catégories importantes composant ce groupe de contaminants est les BTEX (benzène, toluène, éthylbenzène et xylène) qui sont les produits principalement trouvés dans l'eau souterraine suite à une contamination à l'essence. Donc, afin de représenter l'essence altérée par un passage dans le sol, le p-xylène, un des BTEX, a été choisi puisque ses propriétés physicochimiques (Tableau 2.1) sont conservatrices par rapport à celles de l'essence dans un contexte de réhabilitation. La densité et la viscosité du p-xylène étant plus élevées que celles de l'essence, il est donc moins mobile dans un milieu poreux. Sa pression de vapeur étant plus faible que celle de l'essence même lorsqu'altérée, le p-xylène est donc moins volatile. Le choix du p-xylène permet l'utilisation d'un produit pur de grade laboratoire moins volatile et moins toxique que l'essence.

Tableau 2.1 – Propriétés physicochimiques du p-xylène et de l'essence.

Produit Chimique	Densité (kg/m³)	Viscosité (mPa·s)	Pression de vapeur (atm) à 20°C
p-xylène	0.8611[1]	0.644[1]	0.0086[2]
Essence	0.7321[1]	0.45[1]	0.34[2]
Essence altérée*	-	-	0.049[2]

* Telle que définie par Johnson et al. (1990)
[1] Mercer et Cohen (1990)
[2] Johnson et al. (1990)

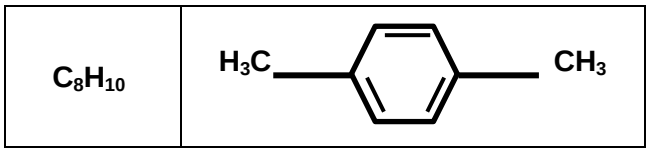

Figure 2.1 – Formules chimique et topologique du p-xylène

2.2 Propriétés des tensioactifs

Les tensioactifs (surfactants en anglais) sont communément appelés détergeants, il s'agit de produits purs ou de mélanges constitués de molécules ayant une tête hydrophile et une queue hydrophobe. Les molécules, lorsque seules, sont appelées monomères. Lorsque la concentration en tensioactif dans l'eau dépasse une certaine valeur appelée concentration micellaire critique (CMC), les monomères peuvent s'agréger en structures appelées micelles. Ces structures sont constituées de plusieurs monomères dont la tête hydrophile est dans l'eau et la queue hydrophobe est orientée vers l'intérieur de la micelle. Il existe toutes sortes de formes de micelles (sphérique, bâtonnets, etc.) et les micelles d'un même tensioactif peuvent varier de forme suivant la concentration.

Les tensioactifs se divisent en plusieurs types suivant la charge ionique de leur tête hydrophile. Les tensioactifs anioniques ont une charge négative, les cationiques positive et les anioniques n'ont pas de charge. Il existe aussi un type de tensioactifs appelé amphotère, ceux-ci peuvent avoir une charge positive ou négative dépendamment du pH. Ces différents types ont des propriétés différentes particulièrement en ce qui a trait à l'adsorption sur les particules de sol.

Lorsqu'il y a présence d'une interface entre le tensioactif dans l'eau et un fluide immiscible, l'air par exemple, les monomères vont partitionner à l'interface en s'orientant de façon à ce que leur tête hydrophile soit dans l'eau et leur queue hydrophobe soit dans l'air. Ils vont ainsi modifier un paramètre appelé la tension interfaciale (σ) ou, lorsque le fluide en contact avec le tensioactif est de l'air, appelé tension de surface. La tension interfaciale est définie comme l'énergie nécessaire pour créer une nouvelle unité de surface à l'interface entre deux fluides non immiscibles. Elle est donc définie par un travail par unité de surface :

$$\sigma = \frac{Travail}{Aire} = \frac{Fdx}{dA} [=] \left[\frac{kg}{s^2}\right] [=] \left[\frac{N}{m}\right] \qquad \textbf{Équation 2.1}$$

Donc, plus la tension interfaciale est petite, plus la force nécessaire pour créer une unité de surface est petite et plus les deux fluides immiscibles sont facilement liables.

La mouillabilité d'un fluide se définit comme la capacité de ce fluide, lorsque présent avec un autre fluide, à adhérer ou à s'étaler sur une surface solide. La mouillabilité s'exprime par l'angle de contact (Θ) d'une goutte en contact avec une surface solide, l'angle de contact mesuré est celui dans la phase aqueuse. Par exemple, dans un système composé d'eau (w), d'huile (o) et d'une surface solide (s), la mouillabilité à l'huile exprime la tendance relative de l'huile à

s'étendre sur la surface solide lorsque baignant dans l'eau. Dans le cas d'un sable de silice, le milieu est hydrophile et donc la mouillabilité est à l'eau ce qui implique que le LI occupe le milieu des grands pores.

2.3 Propriétés des mousses

La mousse est un ensemble composé d'un mélange d'air et de liquide. La phase liquide est continue et au moins une partie de la phase gazeuse est discontinue par la présence de minces films de liquides. Donc, lorsque la partie liquide de la mousse est constituée par une solution tensioactive, les parois des bulles sont constituées d'une double couche de monomères ayant la tête hydrophile dans le liquide et la queue hydrophobe dans l'air. De même, lorsqu'il y a présence de liquide immiscible, l'organisation des monomères demeure la même excepté le fait que les monomères situés sur une des doubles couches ont la queue hydrophobe dans le LI tel qu'illustré à la Figure 2.2. La baisse de tension interfaciale entre la solution tensioactive et le LI peut aussi entraîner la formation de fines bulles de LI qui se logent dans les parois des bulles de mousse, permettant ainsi la mobilisation du LI.

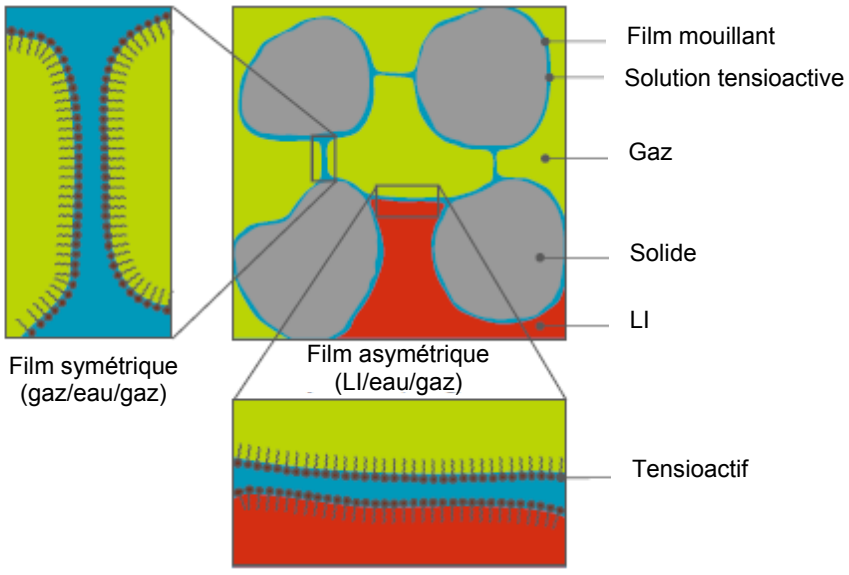

Figure 2.2 – Structure des parois des bulles de mousse, l'air est en jaune, la solution tensioactive en bleu et le LI en rouge. (modifié à partir de Farajzadeh et al., 2012)

La présence de bulles dans la mousse modifie considérablement les propriétés de chacune des phases la composant. Entre autre, en récupération assistée du pétrole (RAP), la viscosité apparente de la mousse peut atteindre 1000 fois la viscosité individuelle de la solution

tensioactive et de l'air (Hirasaki et Lawson, 1985; Manlowe et Radke, 1990). Cette augmentation en terme de viscosité est due à deux phénomènes (Falls et al., 1989) : le cisaillement des parois des bulles entre les parois des pores et l'interface avec l'air et la force nécessaire à appliquer sur les parois des bulles afin de permettre leur passage dans les pores de taille restreinte.

2.4 Forces en présence

Afin de créer un système efficace pour récupérer un LI, il faut d'abord comprendre les forces en présence qui trappent le LI dans les pores :

La force gravitationnelle (ΔP_g) est une force hydrostatique qui dépend du contraste de densité ($\Delta\rho$) entre le LI et l'eau, de la hauteur (h) du LI et de la constante gravitationnelle (g). Dans le cas d'un LIL comme le p-xylène, la force gravitationnelle pousse le LI à migrer vers le haut.

$$\Delta P_g = \Delta\rho g h \qquad \textbf{Équation 2.2}$$

La force capillaire (P_c) résulte de la différence de pression entre deux fluides immiscibles mesurée à l'interface courbe les séparant. Elle dépend de la tension interfaciale entre l'eau souterraine et le LI (σ), de l'angle de contact entre une gouttelette de LI et le sol (θ) et du rayon (r) du pore dans lequel se trouve la gouttelette. La force capillaire retient le LI dans les pores et restreint sa mobilisation.

$$P_c = \frac{2\sigma cos\theta}{r} \qquad \textbf{Équation 2.3}$$

La force visqueuse (P_v) résulte de l'écoulement du fluide déplaçant dans les pores qui pousse le LI dans le milieu poreux. Cette force dépend du flux (q) du fluide déplaçant, de sa viscosité (μ), de la longueur (L) de la gouttelette qui est poussée et de la perméabilité intrinsèque du milieu (k).

$$P_v = \frac{q\mu L}{k} \qquad \textbf{Équation 2.4}$$

La mobilisation d'une gouttelette de LI aura lieu lorsque la force visqueuse dépasse la force capillaire. Le nombre capillaire (N_c) est le rapport entre ces deux forces et donne une indication sur les paramètres pouvant être modifiés afin de mobiliser le LI.

$$N_c = \frac{q\mu}{\sigma cos\theta}$$ **Équation 2.5**

Pennell et al. (1996) ont évalué qu'un nombre capillaire se situant entre $1x10^{-5}$ et $5x10^{-5}$ était nécessaire pour déclencher la mobilisation du TCE dans un sable de silice homogène et qu'un nombre capillaire de $1x10^{-3}$ était nécessaire pour récupérer entièrement le TCE dans les mêmes conditions. Dans cette optique, il est nécessaire d'optimiser le nombre capillaire afin d'augmenter la récupération des LIL par mobilisation.

CHAPITRE 3 : SURFACTANT FOAM SELECTION FOR ENHANCED LNAPL RECOVERY IN CONTAMINATED AQUIFERS

Mélanie Longpré-Girard[a], Richard Martel[a], Thomas Robert[a], René Lefebvre[a], Jean-Marc Lauzon[b]

[a] INRS-Eau, Terre et Environnement, Institut national de la recherche scientifique, Université du Québec, 440 Boul. de la Couronne, Québec, Québec, Canada, G1K 9A9

[b] TechnoRem Inc., 4701 Rue Louis B Mayer, Laval, Québec, Canada, H7P 6G5

Résumé

Cette étude avait pour but d'élaborer une méthodologie permettant le choix d'un tensioactif ainsi que des paramètres d'injection pour la production d'une mousse capable de traiter un sol contaminé au p-xylène. Deux critères de sélection ont été considérés pour le choix du tensioactif : la moussabilité grâce au test Ross Miles et la tension interfaciale avec le p-xylène grâce à la méthode de la goutte pendante. Trois tensioactifs ont été identifiés suite à ces tests : (1) Genapol LRO qui a la meilleure moussabilité; (2) Ammonyx Lo qui a la tension interfaciale la plus basse et qui a la seconde meilleure moussabilité et ; (3) Tomadol 900 qui a été choisi à des fins de comparaisons puisqu'il présente des résultats moyens pour les deux tests. La production de mousse de chacun de ces trois tensioactifs a été testée en colonne et les résultats concordaient avec les essais Ross Miles ; Genapol LRO a produit une mousse si visqueuse que le front est devenu instable à la fin de l'essai alors que Ammonyx Lo a produit une mousse moins visqueuse mais stable tout au long de l'essai, Tomadol 900 a produit une mousse peu visqueuse et instable. Les autres tests en colonne ont permis de déterminer les paramètres d'injection de mousse optimaux afin de produire un front de mousse stable et uniforme : une colonne de production de mousse doit être utilisée, un pré-rinçage de la colonne avec le tensioactif doit être fait avant l'injection de mousse et l'injection de mousse doit se faire à haute pression. Cette étude monte que d'autres essais sont requis afin d'évaluer la stabilité du front de mousse lors d'une injection horizontale dans des dépôts hétérogènes stratifiés.

Abstract

This study aimed to develop a methodology for surfactant selection for foam production and foam injection conditions for the treatment of a p-xylene contaminated soil. Two critera were determined for surfactant selection: foamability evaluated with the Ross Miles test and interfacial tension reduction measured with the Pendant Drop method. Three surfactants were identified following these tests: Genapol LRO because it is producing the highest foam height in the Ross Miles test, Ammonyx Lo which is having the lowest interfacial tension with p-xylene and the second highest foam height and Tomadol 900 for comparison purposes because it had intermediate results in both tests. Foam production of each surfactant was tested in a sand column and results showed the same ranking in foam viscosities than in foamabilities: Genapol LRO produced a foam so viscous that it was destabilized at the end of the experiment, Ammonyx Lo produced a less viscous foam but with a stable front throughout the experiment and Tomadol 900 produced an unstable foam with poor viscosity. The other column tests gave indications on the optimal conditions needed to produce a stable and viscous foam front: a production column must be used, a pre-flush with surfactant solution (having the same concentration and surfactant used in foam) must be done prior to foam injection and injection pressure must be high. This study showed that other tests are needed in order to evaluate the impact of horizontal foam injection through stratified soil layers on foam front behavior.

3.1 Introduction

Many studies on surfactant foam have been carried out in the petroleum industry for the application of foams to enhanced oil recovery (EOR) in deep oil reservoirs (Li et al. 2012a; Farajzadeh et al., 2012; Shallcross et al., 1990). Also, EOR studies often consider fractured sandstone as a favorable porous media for foam injection (Simjoo et al., 2012; Nguyen et al., 2007). However, environmental applications under field conditions are quite different from EOR. Shallow sites contaminated by organic compounds are mainly in unconsolidated porous materials, a low injection pressure must be used to prevent soil heaving and the natural groundwater present in the pores is not saline. Still, few laboratory studies have been carried out to assess foam behavior in porous media for their application to the remediation of shallow contaminated soils (Mulligan and Eftekhari, 2003; Couto et al., 2009, Tanzil et al. 2002a). The application of foams to the remediation of Light Non-Aqueous Phase Liquids (LNAPL) is studied

here, whereas some of the previous work considered Dense Non-Aqueous Phase Liquids (DNAPL), such as TCE, as the contaminant type to be removed (Jeong and Corapcioglu, 2000, 2003, 2005; Rothmel et al., 1998; Pennell et al., 1996). For a DNAPL, mobilization has to be avoided to prevent the sinking of contaminants, which would worsen site contamination. Some field-scale tests of foam injection in shallow soils were also conducted (Hirasaki et al., 2000).

Our study was done in the context of an application of foam to remediate LNAPL-contaminated soils with a specific LNAPL, p-xylene. The objective was to develop a methodology for: (1) the selection of surfactants for foam injection, (2) the ex situ production of foam, and (3) the injection of foam in a sand column in order to observe its behavior in a porous media. This laboratory study was intented to provide a basis to assess the feasibility of such an application of foam for LNAPL-contaminated shallow soils. This paper describes the methodology developed for surfactant selection, foam production and injection, and foam behavior in a 1D sand column.

3.1.1 Enhanced NAPL recovery mechanisms with surfactants and foams

Two recovery mechanisms take place during foam injection for DNAPL remediation: dissolution and volatilization (Mulligan and Eftekhari, 2003). When a LNAPL is treated, however, mobilization can be added to the list and it becomes the main mechanism. To minimize costs, low concentrations of surfactant are used for foam production, which means that enhanced dissolution would be low. LNAPL recovery with volatilization would also be small compared to mobilization because of the limiting factor of transfer from the NAPL phase to the air phase.

NAPL may be mobilized due to the increase of the capillary number (N_c), which is defined as follows (Pennell et al., 1996):

$$N_c = \frac{\mu q}{\sigma cos\theta} \qquad \textbf{Equation 3.1}$$

The increase in viscous forces is achieved by increasing the injected fluid viscosity (μ) and its flux (or velocity) (q) in the porous media, whereas a decrease in capillary forces is possible via a reduction of interfacial tension (σ) by the presence of a surfactant. The wettability is represented by the contact angle (θ). Therefore, maximizing N_c increases the possibility to displace a contaminant with foam. So, each step of this study considered all means to maximize N_c with foam. Replacing water by foam as the displacing fluid in porous media favors NAPL

mobilization because, compared to water, it increases viscosity and decreases interfacial tension by at least one order of magnitude. Interfacial tensions were therefore measured for several surfactants and the best candidates with the lowest interfacial tension with the contaminant were considered for further investigation.

3.1.2 Foam properties

Foam flow through porous media is defined by Hirasaki (1989) as a "dispersion of gas in liquid such that the liquid phase is continuous (i.e. connected) and at least some part of the gas phase is made discontinuous by thin liquid films called lamellae". Foam has non-Newtonian and shear-thinning properties (Hirasaki, 1985; Falls, 1989), which makes foam an alternative solution to the use of polymers for mobility control. Also, the presence of air in foam reduces significantly the amount of surfactant needed to sweep a given volume, compared with surfactant solution injection. Thus, when compared with surfactant solutions, the use of foam can lower the volume of surfactant needed and even replace the use of polymers.

Two conditions were considered in this study to characterize foam-forming surfactants: foamability and foam quality. Foam has dynamic nature, its properties evolving significantly through time. Furthermore, the same surfactant can produce foam with different properties depending on the production method. So, to make sure conditions can be compared between different surfactants, the same foam production method and the same measurement conditions need to be used.

Foam quality is used to evaluate the air content of the foam and is defined by the following expression (Chowdiah et al., 1998):

$$Foam\ Quality = \frac{Gas\ volume}{Total\ volume} \qquad \textbf{Equation 3.2}$$

For the purposes of this study, foamability is considered as the height of foam produced during a Ross Miles Test, as described by Li et al. (2012b). This test involved the use of a fixed volume of surfactant solution that falls in a receiving tube of a certain height into a constant volume of the same surfactant solution.

Foam viscosity cannot be measured with conventional methods because of its dynamic nature. It is therefore necessary to assess the apparent viscosity (μ_{app}) of foam as it flows in a horizontal

1D porous media using Darcy's Law in its generalized form for the flow of any Newtonian fluid (Bear, 1972; Marsily 1986):

$$\mu_{app} = \frac{k\nabla P}{q} \qquad \textbf{Equation 3.3}$$

Where k is the intrinsic permeability (m²), ∇P is the pressure gradient (Pa/m) and q is the volumetric flux (m³/m^2·s or m/s).

3.1.3 Research objectives

The general objective of this study was to develop a methodology for the selection of a surfactant and foam production in order to remediate LNAPL-contamination in soils at shallow depths. The specific objectives of this work were:

- To select a surfactant capable of producing a foam suitable for the remediation of LNAPL-contaminated soils, specifically for p-xylene. This selection is based on the characterization of foam properties (foamability, foam stability, foam quality, foam viscosity);
- To produce foam ex-situ and inject it in a 1D sand column;
- To characterize foam under shallow soils conditions using a sand column (1D) and verify the effects of: injection pressure, pre-flush with water or surfactant solution and surfactant used on foam behavior.

The 1D column used homogeneous clean sand, distilled water and one surfactant solution at a time (no mixtures). The context of field application imposed the use of:

- A low surfactant concentration to lower the costs;
- A low injection pressure to prevent soil heaving;
- A stable foam front to avoid fingering and loss of NAPL during NAPL recovery.

3.2 Methodology

3.2.1 Surfactant selection methodology

Three criteria were considered in order to select the most suitable surfactant for foam production; biodegradability, foamability and interfacial tension. Foamability was measured with the Ross Miles Test (ASTM D1173). Interfacial tensions between surfactants and p-xylene were measured by the pendant drop method (Woodward, 2011). Table 3.1 presents the list of all tested surfactants including their biodegradability. They are all biodegradable, except for Triton X-100 which was tested for comparison purposes

Table 3.1 – List of tested surfactants.

	Surfactant	Molecule Name	CAS number	Type	Active Matter (%)	Supplier	Biodegradability*
A	**Genapol LRO**	Sodium alkyl ether sulfate	68891-38-3	Anionic	68	Clariant	Readily
B	**Ammonyx LO**	Lauramine oxide	1643-20-5	Amphoteric	31	Stepan	Readily
C	**Ammonyx CDO - Special**	Cocamidopropylamine oxide	68155-09-9	Amphoteric	33	Stepan	Readily
D	**Steol CS330**	Sodium laureth sulfate	9004-82-4	Anionic	28	Stepan	Readily
E	**Amphosol CA**	Cocamidropropyl betaine	61789-40-0	Amphoteric	30	Stepan	Readily
F	**Chembetaine CAS**	Cocamidropropyl hydroxy sultaine	68139-30-0	Amphoteric	50	Chemco	96% (Mouton et al., 2009)
G	**Biosoft N1-9**	Ethoxylated alcohol	34398-01-1	Nonionic	100	Stepan	80%
H	**Tomadol 1-7**	Ethoxylated alcohol	34398-01-1	Nonionic	100	Air Products	Readily
I	**Tomadol 900**	Ethoxylated alcohol	68439-46-3	Nonionic	100	Air Products	Readily
J	**Biosoft N23-6.5**	Ethoxylated alcohol	66455-14-9	Nonionic	100	Stepan	80%
K	**Triton X-100**	Octylphenol ethylene oxide	9002-93-1	Nonionic	100	Sigma-Aldrich	Not readily
L	**Biosoft N91-8**	Ethoxilated alcohol	68439-46-3	Nonionic	100	Stepan	80%
M	**Polysorbate 80**	Polyoxyethylene sorbitan monooleate	9005-65-6	Nonionic	89	Croda	Readily

* According to supplier datasheet.

Foamability

The Ross Miles Test (ASTM D1173 method) quantifies both the capacity to produce foam and its stability under standardized conditions. This method is used to compare surfactants that produce foam, it does not measure any intrinsic property and needs to be used under the same conditions for all tests. All surfactants were tested at these concentrations: 0.01%, 0.1% and 1% w/w.

A standard apparatus is needed to carry out the Ross Miles Test (Figure 3.1). This apparatus consists of a glass receiver and a 200 ml glass pipet (Wilmad LabGlass, New Jersey). The methodology is as follows: (1) the walls of the receiver are rinsed with distilled water in order to clean any remaining surfactant; (2) the stopcock at the bottom of the receiver is closed and the walls are rinsed with 50 ml of the surfactant solution, which remains at the receiver bottom; (3) the pipet is placed on top of the receiver. The receiver height is standardized so the bottom of the pipet is exactly at a 90 cm height of the 50 ml line; (4) the pipet stopcock is opened, which allows the surfactant solution to fall into the 50 ml of surfactant solution already at the bottom of the receiver; (5) foam is produced by the solution's drop; (6) when all the solution has run out, a measurement of foam height is taken at t=0 min and a stopwatch is started and further measurements are taken at times of 1, 3, 5 and 15 minutes.

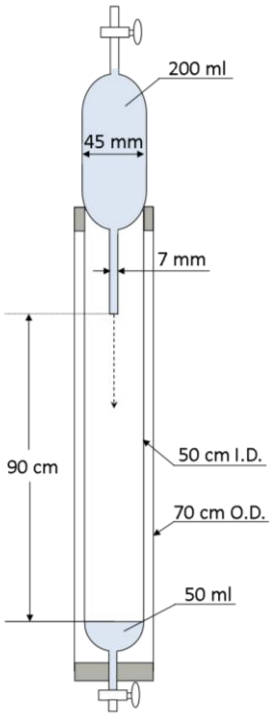

Figure 3.1 - Apparatus used for the Ross Miles Test.

This method has the following advantages: each test is done in a short period of time, it is repeatable and the apparatus height allows neglecting the effect of humidity. As reported by Li et al. (2012b), the distance between the top of the foam and the receiver top opening is crucial for the humidity gradient over the foam, which has an effect on foam collapse. When the humidity gradient is low, the evaporation rate is also low and the foam is more stable.

Considering that the best foam tested reached a height of 18.6 cm and the receiver total height of 90 cm, a distance of 71.4 cm was considered sufficient to have negligible evaporation. However, this technique does not consider the change in foam quality through time, only the foam height. Therefore, even if most of the liquid contained initially in the foam has drained out and the bubbles are large and unstable, foam height can still remain the same as initially measured. Bubbles can collapse and all the liquid is drained down or bubbles can join and form bigger bubbles that will remain in place. Therefore, measurements of foam height through time are not good indications of foam stability; thus measurements through time were not considered for the present study.

Sometimes, bubbles become bounded to the glass walls and create a higher concentration of bubbles near the walls that stabilize them. A hole in the middle of the receiver is apparent. When it occurred, measurements of foam height were made where it appeared continuous through the width of the receiver.

Interfacial tension

Interfacial tensions between surfactant solution and p-xylene were measured with a FTA 200 Dynamic Contact Angle Analyzer from First Ten Angstroms, which uses the pendant drop technique. Images are taken of a p-xylene drop injected upside down with a “U” shaped flat ended needle (0.356 mm diameter) in a glass cell filled with the tested surfactant at concentrations of 0.01%, 0.1% and 1%. A computer activated pump controls p-xylene injection. A p-xylene drop needs to be large enough to be distorted by gravity as interfacial tension tries to balance this distortion. Interfacial tension (IFT) is assessed by fitting the shape of the drop to the Young-Laplace equation. The captured video image was calibrated with phase densities and with the size of the needle tip. FTA35 software was used to treat drop images and compute IFT values.

3.2.2 Foam production and injection system

Many foam production methods were tested, including: injection at constant rate with syringe pumps, injection with a porous stone in a foam production column and alternating injection of surfactant and air at the same pressure in a foam production column. The first two methods did not perform well because no foam was produced by either method. Indeed, when tested in the laboratory, these methods only produced alternate slugs of air and surfactant solution. The latter method was selected because a constant flow of foam was easily produced and foam quality was easily measurable. Furthermore, foam production at a constant pressure has been reported to be more efficient than production at a constant rate (Li, 2011).

A stainless steel tank (6.6 L, 18 cm diameter, 26 cm height, 5 mm thick) was filled with surfactant solution and connected to the pressurized air line controlled by a pressure regulating valve (0.64 cm diameter, 300 psi, Parker) (Figure 3.2). Then, both air and surfactant solution lines were connected to two valves (0.5 cm diameter, shutoff valve 104R, Asco) that opened alternatively at fixed times steps. This setup allowed air and surfactant solution injection at the same pressure.

After initial tests, it appeared that alternating times had no significant effect on foam production, so it was decided that fixed times were to be used for all further testing: five seconds of surfactant solution injection alternating with ten seconds of air injection. Those short periods of time were selected because they created only small variations in the injection pressure signal and thus in the pressure transducer response. Also, heating of the electric valves favored short alternate opening of each valve. After flowing through the valves, air and surfactant solution are mixed in a ‘’T’’ shaped tube and then go through a foam production column, which is an acrylic column filled with 2 mm diameter glass beads with 250 µm opening screens between each 2.5 cm glass bead layers. This column allowed the purging of foam until it was stable and the measurement of its quality before it entered the sand column. This procedure only allowed already pressurized stable foam to enter the sand column.

When foam exiting the production column had a stable quality, it was flowed through the glass sand column and filmed at a high resolution with a digital camera (Nikon, Coolpix P510). As shown on Figure 3.2, four pressure transducers were also placed at key positions throughout the system, to measure changes in pressure along the production system: one at the foam production column inlet (T-1), one at the sand column inlet (T-2), one in the upper and lower ports in the sand column (T-3 and T-4). The line carrying the effluent was placed at a fixed

height of 5 cm above the sand column inlet to maintain a back pressure at the outlet of the column. The next section further describes sand column experiments.

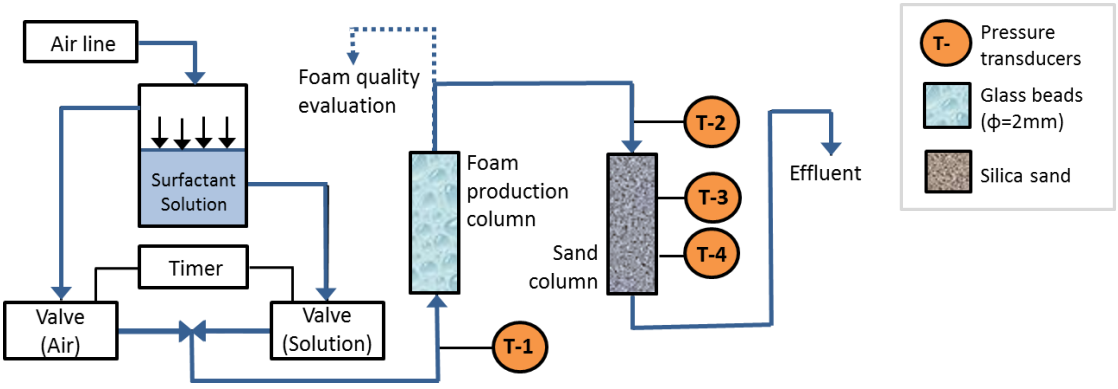

Figure 3.2 - Experimental setup for foam production and injection into sand columns. T-1 through T-4 refer to pressure transducers. Videos were made of foam flow through the transparent acrylic sand column.

3.2.3 Sand column experiments

Sand column experiments are a first step towards the assessment of the suitability of foam for LNAPL remediation, prior to laboratory sand box experiments and field pilot-testing. Sand column tests were designed to help understand the effects of different variables on foam flow through soils, especially pre-column use, injection pressure, surfactant concentration, pre-flush liquid and surfactant types. Sand column experiments were done with the three more suitable surfactants selected following foamability tests and interfacial tension measurements described previously.

Silica sand (99.9% quartz) was used for all experiments in order to minimize fines (clay and silt) and organic matter contents of soils and the interaction of surfactant with other minerals. The same silica sand was used for all tests, which was Temisca 20 (Opta Minerals Inc.), a coarse sand whose properties are listed in Table 3.2.

Table 3.2 – Properties of Temisca 20 sand used in column experiments. d_{10} and d_{50} refer to grain sizes larger than 10% and 50%, respectively, of sand mass.

d_{10}	d_{50}	Permeability	Hydraulic conductivity
0.75 mm	1.3 mm	$4x10^{-11}$ m²	$4x10^{-4}$ m/s

Sand filling and compaction in columns were done as described by Martel and Gélinas (1996). Columns are made up of a transparent acrylic cylinder with a 3.5 cm internal diameter and a

14.5 cm length. Acrylic was selected for its resistance to compression and its transparency, which allowed the filming of foam flow. Both ends are sealed with a perforated Teflon cap combined with a reservoir that uniformly distributes fluids before their entry into the sand column. The seal between the acrylic cylinder and the Teflon caps is provided by a Viton O-Ring. A nylon screen (125 µm mesh) on each Teflon cap prevents the loss of sand through the perforated caps. Two holes were pierced on the side of the column to connect pressure transducers and the same nylon screen was placed on each hole to prevent sand loss.

Compaction of each 5 mm sand layers was done by dropping a 500 g weight 12 times from a height of 8 cm. The top surfaces of compacted layers were lightly scarified to minimize preferential flow paths between subsequent layers. The sand column had a global dry density of 1.64 g/cm³ which is enough to prevent channeling that may occur below 1.6 g/cm³ (Ripple et al., 1973). Trapped air in column was eliminated by circulating at least 30 pore volumes of CO_2 through the column. Then the column was saturated from the bottom up with degased distilled water in which CO_2 solubilizes. At least 3 pore volumes (PV) of water were circulated through the sand column in order to flush or solubilize all CO_2. The same column was used for every tests mentioned in this study in order to produce comparable experiments. After each test, the column was rinsed with water and dried with compressed air. It was then purged with CO_2 and saturated again with degassed distilled water.

The effects of four conditions were tested in column: the use of a foam production column, pre-flush with surfactant or water, the use of different solubilized surfactants and the injection pressure.

The effect of the foam production column was tested by making two tests: one with a foam production column and one without. Both tests were done with the same conditions except that one test was done without a foam production column. This test was done as follows: pressurized surfactant was injected first and then air was injected in the sand column after the completion of surfactant solution injection. So, in this test, foam was produced inside the column whereas it was produced in the foam production column in the other test. The effect of the pre-flush liquid was tested by making two tests: one with a column pre-flushed with water and one with a column pre-flushed with surfactant prior to foam injection. Both tests were done with the same foam injection conditions. The effect of the use of different surfactants was tested by making three tests, each with a different surfactant solution chosen following Ross Miles test and Pendant Drop test results. These three tests were done with the same foam injection conditions. The effect of injection pressure was tested by making two tests: one at a lower

injection pressure and another with a higher injection pressure. Other than injection pressure, both tests were done with the same foam injection conditions.

Foam apparent viscosity measurements were done for each column test in order to evaluate the effect of each parameter previously mentioned. They were estimated via foam flow rate and pressure measurements. Injection pressure was fixed for each test and pressure throughout the setup was measured with pressure transducers (T-1 through T-4) positioned as shown in Figure 3.2. Flow rate was calculated with two indirect methods: the velocity of the foam front (Front Velocity Method) and the foam flow rate at the system outlet (Output Method). The Front Velocity Method involved the measurement of the foam front velocity when it passed the second pressure transducer in the column. Apparent viscosity was calculated using the pressure gradient between the two pressure transducers (T-3 and T-4) in the column at that time. This method provides an evaluation of foam viscosity at the beginning of the column test, before the column is completely swept by foam. The Output Method used foam rate measured at the column outlet after a certain time of foam injection, when the pressures measured in the column had stabilized. For this method, apparent viscosity was calculated using the stabilized pressure gradient between the two pressure transducers (T-3 and T-4) in the column and the measured flow rate at the column outlet. This method provides a stabilized measurement of foam viscosity at the end of the experiment.

3.3 Results

3.3.1 Surfactant selection

Foamability

Figure 3.3 presents foamability indicated by the initial foam height of the Ross Miles Test for all surfactants tested. Surfactants have been placed in decreasing order starting from the best to worst foamability at 0.1% surfactant concentration (red columns). Considering the small changes in foamability between concentrations of 1% and 0.1% for the best surfactant candidates and the large impact of surfactant cost on potential future field applications, the concentration used for column testing was fixed at 0.1%. Concentrations of 0.01% generally produced quite lower foamability and unstable foam that collapsed quickly. They were thus not considered for comparisons.

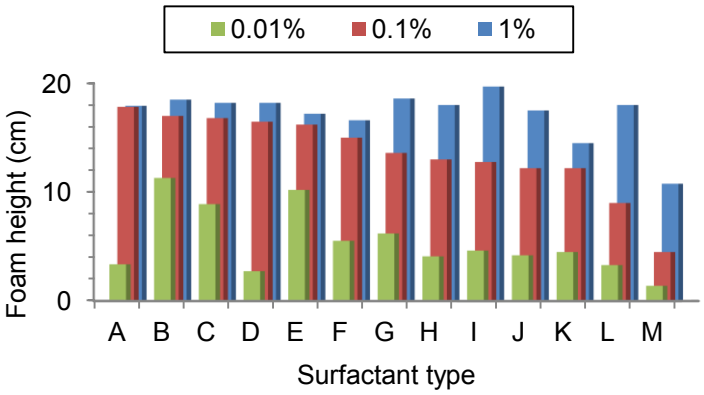

Figure 3.3 –Foamability of surfactant solution at concentrations of 0.01%, 0.1% and 1% measured with the Ross Miles Test for all tested surfactants (A through M; see Table 3.1).

Interfacial tension

Interfacial tension is a key parameter for the evaluation of potential NAPL dissolution and mobilization. In order to maximize the capillary number for mobilization, the interfacial tension between the NAPL and surfactant solution has to be minimized. Figure 3.4 shows interfacial tensions between p-xylene and the surfactant solutions tested. Surfactants were placed in order of increasing interfacial tension at a 0.1% w/w concentration. Surfactant B would provide the best mobilization because it lowers interfacial tension with the NAPL by two orders of magnitude compared with water.

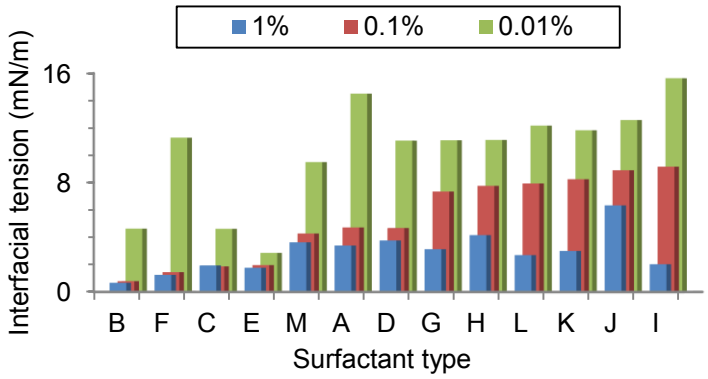

Figure 3.4 - Interfacial tension between p-xylene and the tested surfactant solutions at concentrations of 0.01%, 0.1% and 1% (A through M; see Table 3.1Table 3.1).

Considering pendant drop and Ross Miles test results, three surfactants (A, B, and, I) were selected to be further studied in column tests (Figure 3.5 and 3.7). Surfactant A has the best foamability but has an interfacial tension with p-xylene higher than surfactant B, which shows

the lowest interfacial tension. Surfactant I presents worse results in both tests than the other two surfactants, but it was selected to provide a comparison of the performance that can be obtained with a poor foaming agent. Considering those comparisons, surfactant B was expected to be the best surfactant for p-xylene remediation purposes. Surfactant B was thus selected to carry out for p-xylene remediation purposes. Surfactant A and B were thus selected to carry out column tests aiming to show the influence of different conditions.

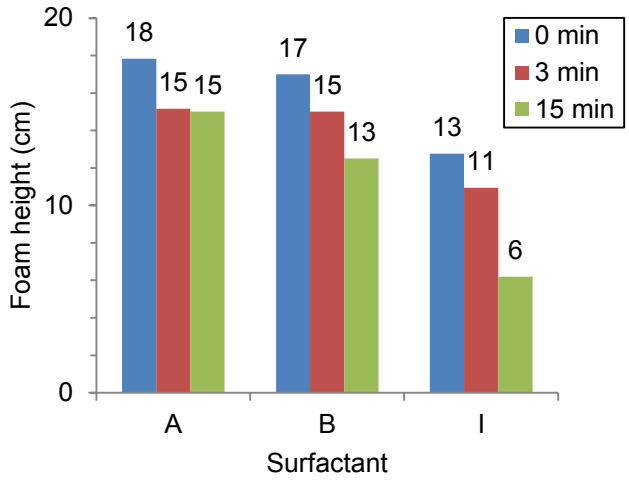

Figure 3.5 - Foamability expressed as foam height (cm) of selected surfactant solutions measured with the Ross Miles Test at three different times at 0.1% concentration.

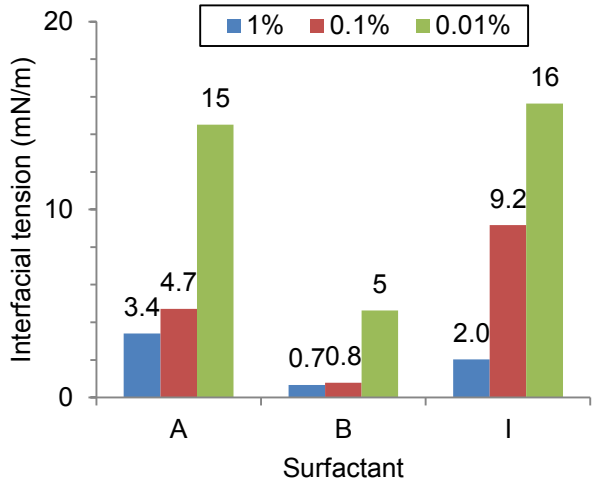

Figure 3.6 - Interfacial tension (mN/m) between p-xylene and the selected three different surfactant solutions at 0.01%, 0.1% and 1% concentrations.

3.3.2 Sand column tests for the effect of various conditions

Several tests were carried out to compare the effect of various conditions on foam flow in a sand column: the effect of foam production column use, pre-flush liquid, surfactant solution used and injection pressure. Table 3.3 summarizes all types of columns tests carried out in this study. Table 3.4 summarizes which column tests were used to evaluate each parameter studied in this work.

Table 3.3 – Summary of column tests including the characteristics of each test, a concentration of 0.1% w/w was used for all tests.

Test Number	Foam production column	Pre-flush Liquid*	Surfactant	Injection pressure (cm H_2O)
1	Yes	SS	A	350
2	No	SS	A	350
3	Yes	SS	B	350
4	Yes	W	B	350
5	Yes	SS	I	350
6	Yes	SS	B	210

* SS stands for surfactant solution and W for water.

Table 3.4 – Summary of the conditions evaluated with the corresponding column tests and figures.

Parameter evaluated	Figure	Tests compared		
Effect of foam production column presence	Figure 3.7	1	2	
Pre-flush with water or surfactant	Figure 3.9	3	4	
Use of surfactant solution A, B or I	Figure 3.12	1	3	5
Injection pressure	Figure 3.14	3	6	

Effect of a foam production column on foam stability

This test was done to verify if the use of a foam production column before the injection of foam in the porous media (represented by a sand column) may increase the foam apparent viscosity. So, a test was done with (Test 1) and without (Test 2) a foam production column. Since foam is injected at the same pressure (350 cm water) in both cases, viscous foam will advance more slowly in the column. Photos of the advancing foam front are shown in Figure 3.7 and it clearly indicates the velocity (and thus viscosity) of the injected foam.

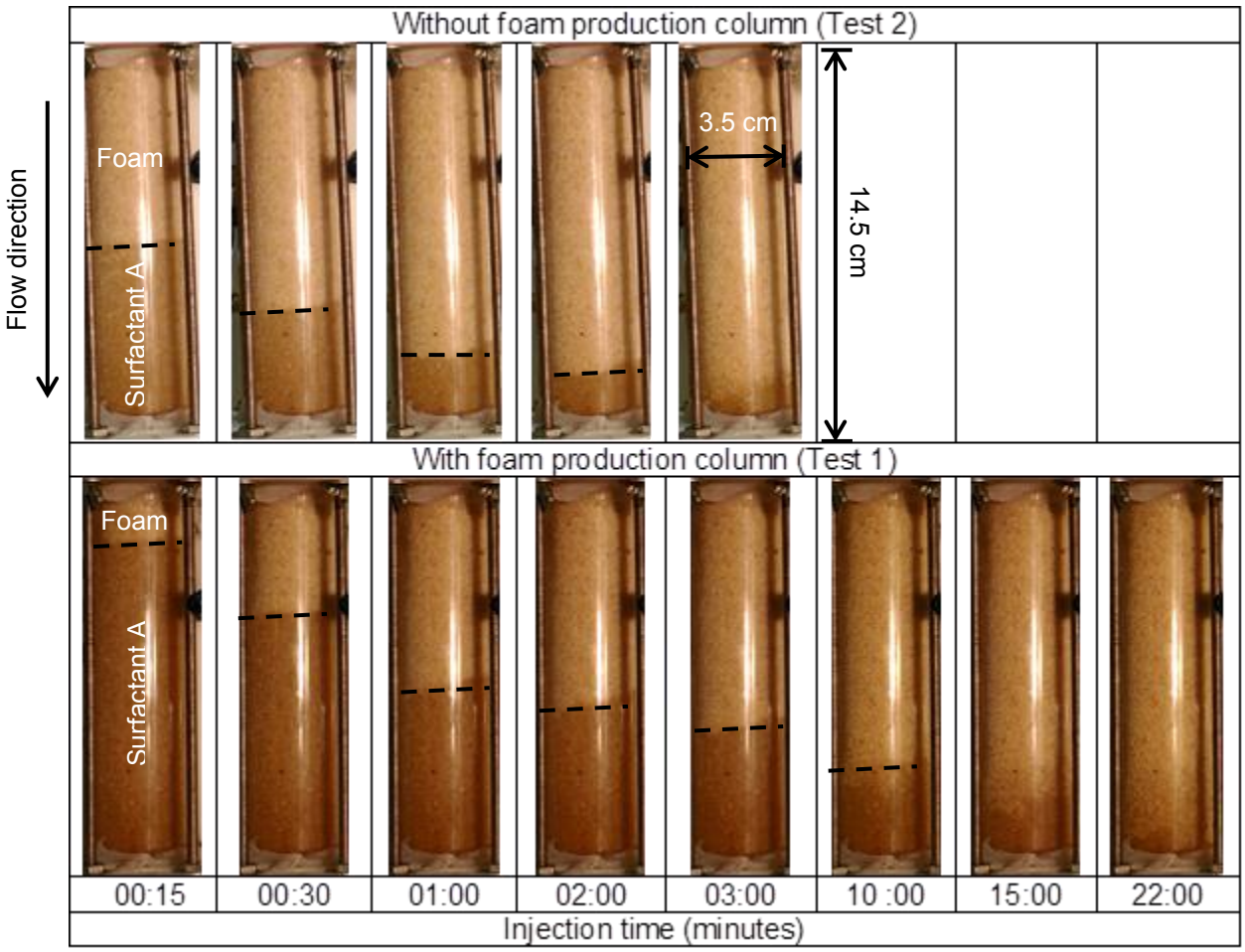

Figure 3.7 - Advancing foam front of surfactant A (0.1% w/w concentration) injected downward following a surfactant pre-flush at a constant pressure of 350 cm water in a Temisca 20 sand column with and without a foam production column. The black dotted line indicates the foam front position.

Figure 3.7 indicates that the front in the test without a foam production column (top) moved significantly faster than in the test with a foam production column (bottom). This thus indicates a greater foam viscosity when a foam production column is used compared to the test without foam production column. Both experiments involved the formation of a strong foam with a stable water displacement front. Evaluation of viscosity with the Front Velocity method indicated a value of 8 mPa·s without a foam production column and 338 mPa·s with it (Figure 3.8). When the foam front passed the second pressure transducer, it was a lot more viscous in Test 1 than in Test 2. With the Output Method, viscosity estimates were 204 mPa·s without foam production column and 254 mPa·s with it. These results are in the same order of magnitude so, when foam has stabilized and pressure is constant, both foam production methods tend to have similar apparent viscosity. Still, viscosity is significantly higher when a foam production column is used.

Considering these results, the following tests were done with a foam production column in order for the foam to stabilize more quickly and be more viscous.

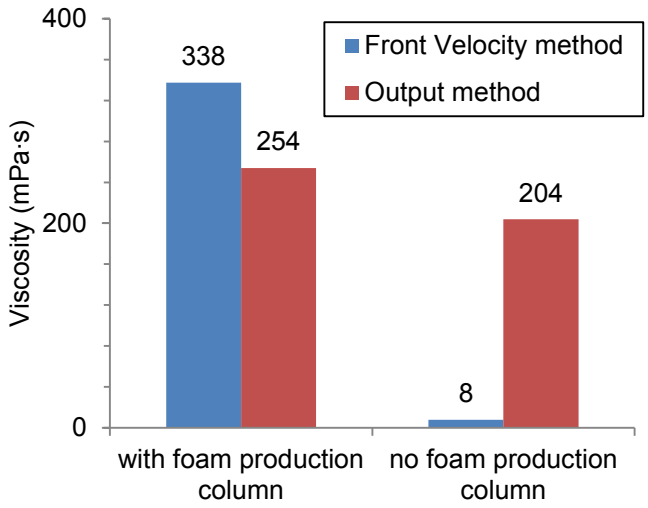

Figure 3.8 – Calculated foam viscosity (mPa·s) of foam produced with 0.1% concentration surfactant A solution in sand column with and without a foam production column using the Front Velocity and Output methods.

Effect of water or surfactant pre-flush

The sand column must be pre-flushed with a liquid prior to foam injection to be representative of saturated conditions as found in the field. Two scenarios with water (Test 4) and surfactant solution (Test 3) as pre-flush liquid were tested with surfactant B at a concentration of 0.1% and a foam injection pressure of 350 cm H_2O in the sand column.

Figure 3.9 shows that, with surfactant pre-flush, a straight uniform front formed, indicating the formation of a strong foam. For the water pre-flush experiment, there is formation of a first blurred foam front with poor sweep and then a second front with more viscous foam that advances more slowly and with better sweep efficiency. However this second front and the front observed in surfactant pre-flush experiment take the same time to sweep entirely the column, thus indicating that foam viscosity is similar. In order to evaluate apparent viscosity with the Front Velocity Method in the sand column test with water pre-flush, the second front which was more clearly defined was selected. Figure 3.10 shows the apparent foam viscosities estimated with the Front Velocity and Output methods, which confirm that foam viscosity was almost identical with the two types of pre-flush fluids.

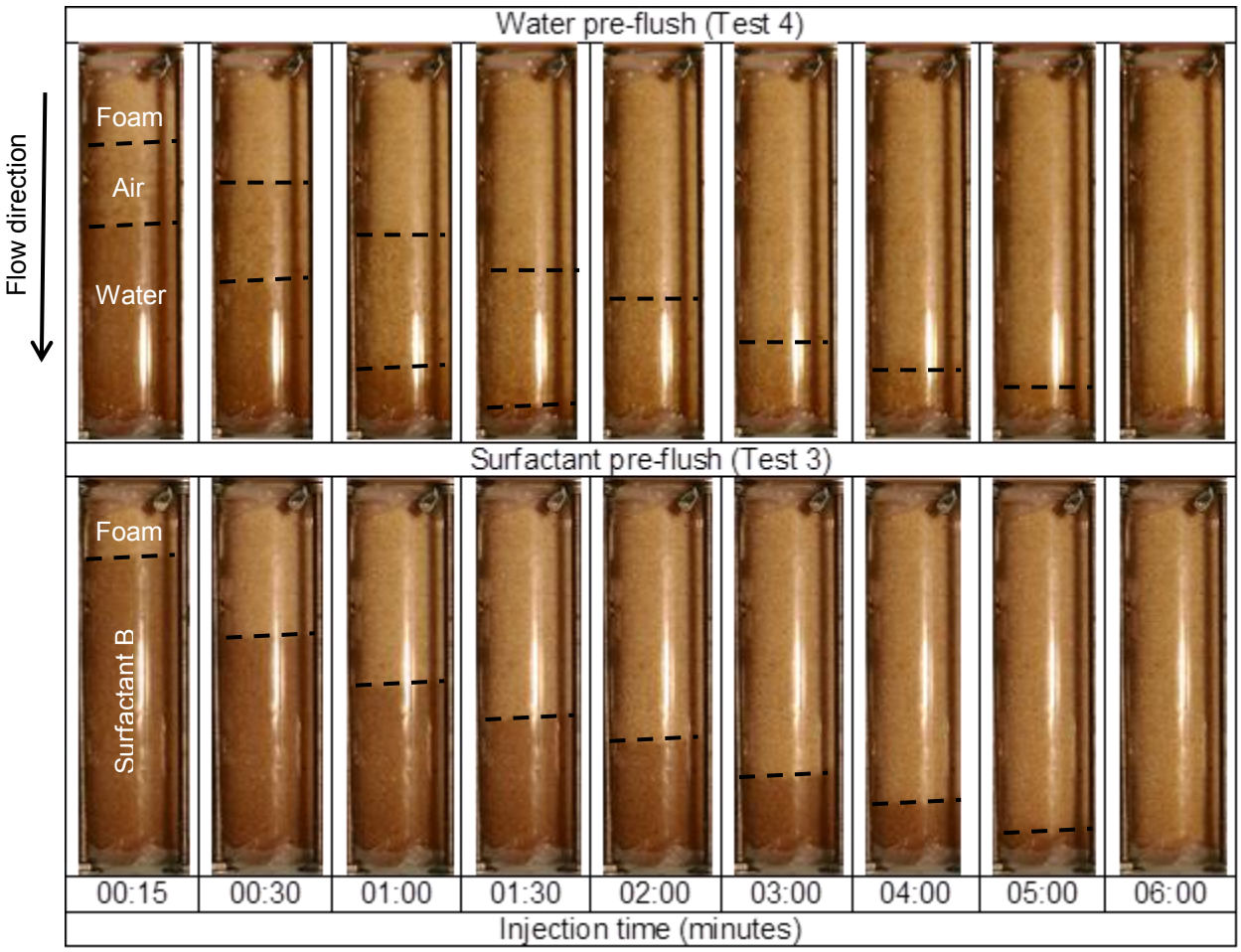

Figure 3.9 - Advancing foam front of surfactant B injected downward at a pressure of 350 cm H2O in the sand column pre-flushed with water or liquid surfactant as a function of time (minutes). The black dotted line indicates the foam front position.

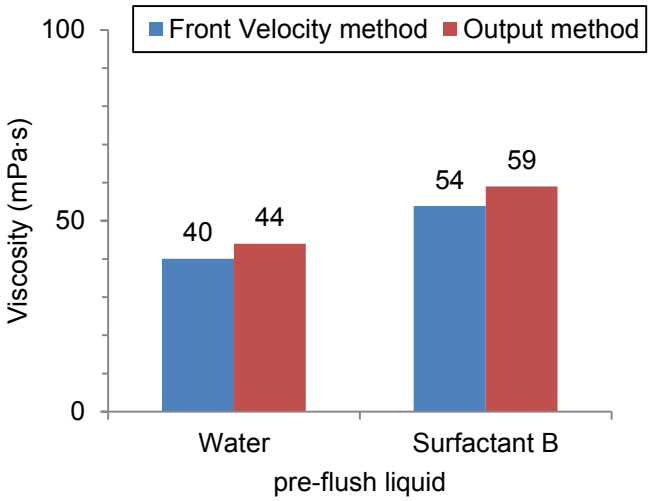

Figure 3.10 – Calculated 0.1% concentration surfactant B solution foam viscosity in sand column when pre-flushed with water or liquid surfactant using the Front Velocity and Output methods

Figure 3.11 shows each front velocity through time before they attained the column outlet. The second front with water pre-flush and the front with surfactant pre-flush both show similar advancing behavior which indicate similar viscosities as injection pressure was stable throughout the experiments. Viscosities calculated with both methods are similar for both tests (Figure 3.10). They indicate that pre-flush with water or surfactant solution does not significantly affect foam viscosity. Therefore, it was decided that all further experiments would be done with a surfactant pre-flush in order to create an easily observable and stable foam front.

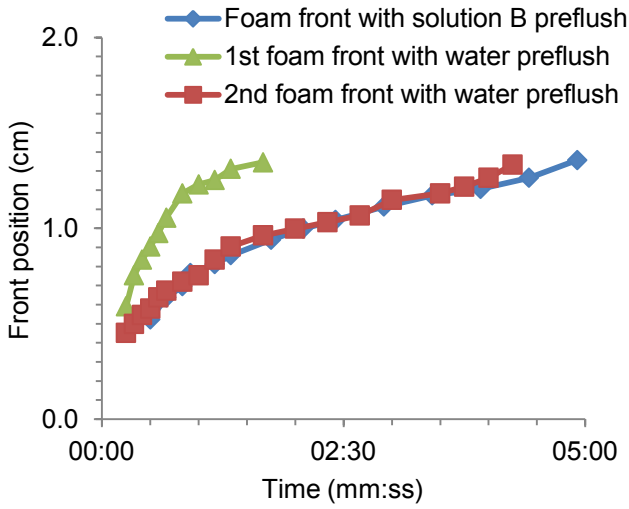

Figure 3.11– Foam front velocity of surfactant B solution 0.1% foam injected in Temisca 20 sand column pre-flushed with water or surfactant solution B 0.1%.

Effect of surfactant type

Figure 3.12 compares the position of foam fronts for 0.1% concentrations of surfactants A (Test 1), B (Test 3) and I (Test 5) injected at pressures of 350 cm of water in the sand column. It shows that surfactant I has a foam front much faster than the two others; the slowest being surfactant A. Also, the front becomes unstable at the end of foam injection in sand column with surfactant solutions A and I.

Figure 3.13 shows the estimated viscosities of these foams. Surfactant A is the most viscous and is followed by surfactant B and surfactant I. Therefore, the ranking of surfactants based on the foamability with the Ross Miles Test (Figure 3.5) is respected, which indicates that this simple test can provide representative indications on surfactant foamability in columns. However, surfactant A produced foam so viscous that the pressure gradient in the column was too large and the front became unstable before the complete sweep of the column (Figure 3.12).

Foam viscosity even dropped during the pressure stabilization in the column, which explains the drop between the two calculations of viscosity in Figure 3.13. Based on these results, it was decided that surfactant B would be used for further testing.

Figure 3.12 - Advancing foam front of surfactants A, B and I (at a concentration of 0.1%) injected with a foam production column downward at a pressure of 350 cm H_2O in a sand column pre-flushed with their respective surfactant solution. The black dotted line indicates the foam front position.

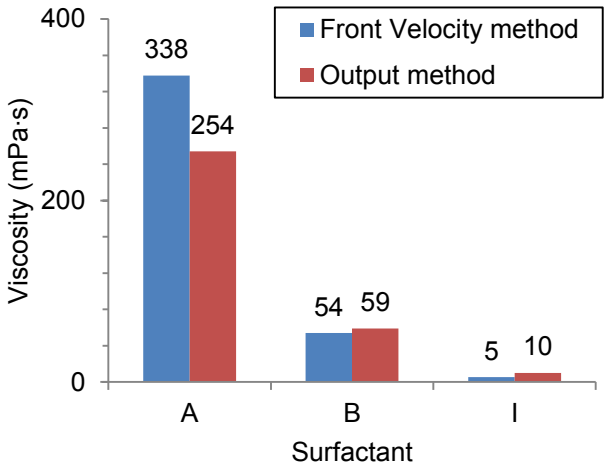

Figure 3.13 - Calculated foam viscosity in Temisca 20 sand column injected with surfactants A, B and I.

Effect of injection pressure

Further column tests were done with surfactant B solution at a concentration of 0.1% at two different injection pressures: 210 cm H_2O (Test 6) and 350 cm H_20 (Test 3). These tests aimed to determine if a lower injection pressure, more suitable for field conditions, could be used and still maintain foam stability and viscosity. An injection pressure of 350 cm H_2O produces a significantly more viscous and more stable foam front than injection at 210 cm H_2O (Figure 3.14). Moreover, a higher injection pressure produces foam that stabilizes and gains viscosity through time as shown in Figure 3.15 by the increasing gap between viscosities estimated at the beginning of the test with the Front Velocity method and at the end of the test with Output method.

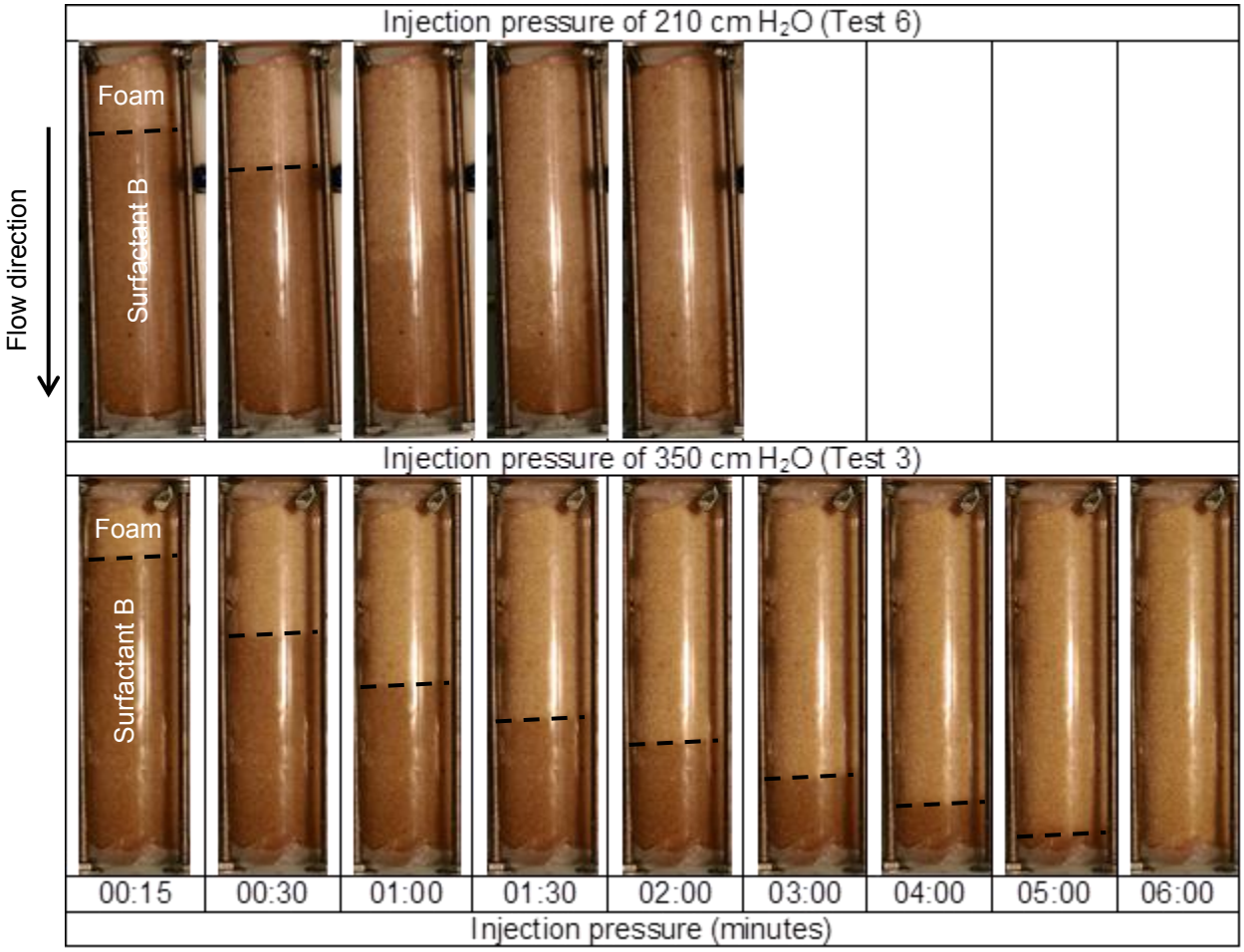

Figure 3.14 - Advancing foam front of surfactant B solution 0.1% injected downward at pressures of 210 and 350 cm H_2O in the sand column pre-flushed with surfactant B solution as a function of time (minutes). The black dotted line indicates the foam front position.

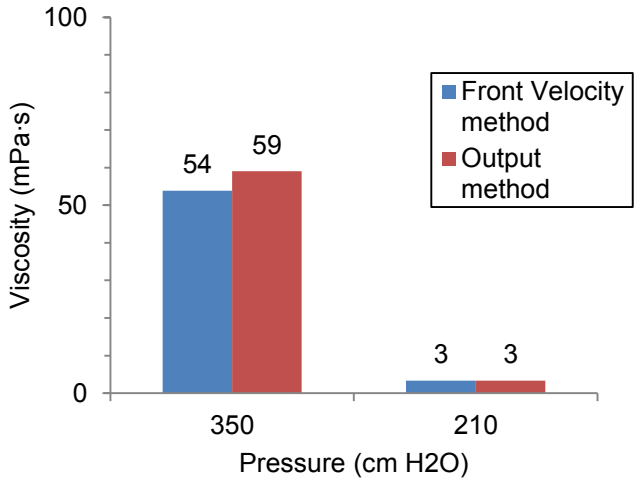

Figure 3.15 - Calculated foam viscosity in sand column with 0.1% concentration surfactant solution B injected at pressures of 350 and 210 cm H_2O.

3.4 Discussion

For surfactant selection, the Ross Miles Test and the pendant drop technique are two simple and quick methods to evaluate surfactant foamability and interfacial tension, respectively. They are two key conditions for the selection surfactant for LNAPL remediation with foams. Column test were in agreement with those of the Ross Miles Test for the three surfactants, as the surfactant solution with the best foamability in Ross Miles test had the most viscous foam front, whereas the one with the worst test had the least viscous foam front. So, Ross Miles test can be used as a screening tool for foam selection. Also, the other foam selection criteria based on the lowering of interfacial tension helps maximize the capillary number but it does not indicate the behavior of foam when in contact with contaminants. In this study, surfactant selection was only based on Ross Miles Test and interfacial tension measurements. The contribution of each type of measurement is unclear on foam behavior when in contact with p-xylene. A third test evaluating the direct effect of p-xylene on foam could complete the list of criteria for surfactant selection. This test would measure the production and collapse of foam without contact with contaminant and when contaminant is mixed with surfactant solution prior to foam formation therefore quantifying the effect of contaminant on foamability as presented by Simjoo et al. (2012).

Table 3.5 – Summary of column test results and conclusions.

Parameter tested	Results		Conclusions
	Negative	Positive	
Effect of foam production column	Without foam production column, foam front is blurred and viscosity is low	With foam production column, foam front is clear and viscosity is high	Foam production column will be used for further testing
Pre-flush liquid	Water pre-flush creates an air front with poor sweep efficiency before the foam front	Surfactant pre-flush creates a clear and stable foam front	Surfactant pre-flush will be used for further testing
Surfactant solution	Surfactant A created a strong foam that was destabilized at the end of the test and surfactant I created a front with poor viscosity	Surfactant B created a clear and stable foam front	Surfactant B will be used for further testing
Injection pressure	An injection pressure of 210 cm H_2O created an unstable foam front with poor viscosity	An injection pressure of 350 cm H_2O created a clear and stable foam front	High injection pressure will be used for further testing

Column tests gave good indications on foam flow conditions in a 1D homogeneous porous media. The objective of those tests was to determine which conditions would allow the production of a stable and viscous foam front. First, the use of a foam production column helped to create a stable foam front with a high viscosity whereas without it, the front was unstable and the initial viscosity was low. However, when pressure stabilized through the length of the column, both systems produced similar viscosities. Therefore, a foam production column was used for further testing in order to make the most stable and viscous foam front possible. Then, the pre-flush liquid was tested in order to determine which liquid between surfactant solution and water would allow the production of a stable foam front. In both tests, the foam front had similar viscosities. However, the front produced in the column pre-flushed with water was unclear due to the presence of a first blurred front with poor viscosity and sweep efficiency. For this reason, surfactant solution pre-flush was used for further testing in order to produce a clear front with good sweep efficiency. Also, the two best surfactant solutions and an average surfactant solution according to Ross Miles test were tested in column. Surfactant solution A created a foam front that was so viscous that it became unstable at the end of the column test. Surfactant solution I produced an unstable foam front with low viscosity whereas surfactant solution B produced a foam front that was viscous and stable through all the length of the column. So, surfactant solution B was chosen for further testing. Finally, injection pressure was tested at 210 and 350 cm H_2O. The injection pressure of 210 cm H_2O produced an unstable foam front with poor viscosity and the injection pressure og 350 cm H_2O produced a stable foam front with high viscosity. A pressure of 350 cm H_2O was therefore used for further testing. Those conclusions gave indications on the design and settings used in a follow up study done with a 2D sandbox made of two sand layers of different grain sizes in order to evaluate mobility control achieved by foam when injection is parallel to the stratification. This study is discussed in the next chapter.

The viscosities evaluated in this section are for comparison purposes only. The filters placed at both ends of the sand column had an opening too small for the sand grain size. Therefore, the permeability was inaccurate due to the flow restriction caused by the small openings of the filters when compared with the flow restriction caused by the sand itself. However, the permeability being the same for all column tests as they were all done in a single sand column, the conclusions remain the same. Also, a problem with the Output Method was that a minimum of 5 ml of foam was needed and it took on average several minutes to collect that volume. A small flow rate combined with the fact that foam collapses through time made difficult the accurate measurement of foam flow. So, when foam viscosity was very high, with surfactant A,

foam flow rate was very low and the measurement of foam flow rate was difficult because of not enough foam exiting the column. In this case, foam flow was underestimated, which increased calculated viscosity compared to reality. Also, when viscosity was very low, with surfactant I, foam tended to collapse faster than in other tests. This often produced slugs of air mixed with foam at the column outlet, which could not be monitored or included in foam flow rate measurements. However, those slugs were clues that this foam had a poor stability. All those considerations indicate that all measurements made with the Output Method underestimated the volume of foam coming out of the column and therefore overestimated foam viscosity.

Still, an injection pressure of 350 cm H_2O for a 15 cm long homogeneous coarse sand column does not provide a realistic representation of expected field scale behavior with heterogeneous sand with a low permeability. More work needs to be done in order to minimize injection pressure to produce a stable front.

3.5 Conclusions

The general objective of this study was to develop a methodology for the selection of a suitable surfactant to make foam used for the remediation of LNAPL-contaminated shallow sediments. Surfactant solutions were tested to compare their foaming properties with the Ross Miles test and their interfacial tension with p-xylene using the pendant drop method. Three surfactants solutions were chosen and tested in 1D homogeneous sand column. Column tests were also done to evaluate injection conditions needed to obtain a stable and viscous foam front such as: the use of a foam production column, column pre-flush with either water or surfactant solution prior to foam injection and injection pressure.

The Ross Miles test proved to be suitable for the identification of surfactant solutions having good foaming properties. Column tests indicated that the surfactant solution with the best foamability in Ross Miles test (Genapol LRO) formed a more viscous foam front during column injection compared to the surfactant solution with less foamability (Ammonyx Lo). Also, the surfactant solution with the worst foamability of the three (Tomadol 900) presented an unstable front with poor viscosity. The Ross Miles test being simple and fast to execute, it is an interesting tool to rank surfactant solutions in terms of foaming ability. The other column test gave indications on conditions to consider for foam injection in further studies: a high injection pressure, the use of a foam production column and the column pre-flush with surfactant solution prior to foam injection.

The tests reported in this study for surfactant selection and foam behavior observed in column are only the first steps towards the field application of surfactant foam injection to remediate LNAPL-contaminated shallow soils. Other tests are needed to evaluate the impact of horizontal injection through soil layers on foam front behavior. A follow up study using 2D sandbox tests carried out for this purpose with a surfactant having the optimal behavior on the basis on this paper is reported in the next chapter.

3.6 Acknowledgements

Funding of this study was provided by a NSERC-CRD grant in partnership with TechnoRem and a NSERC-discovery grant of Richard Martel. The authors would like to gratefully acknowledge the donation of surfactant samples by Stepan and the help of M. Luc Trépanier form INRS in designing and installing the foam injection system.

CHAPITRE 4 : 2D SANDBOX EVALUATION OF FOAMS FOR MOBILITY CONTROL AND ENHANCED LNAPL RECOVERY IN LAYERED SOILS

Mélanie Longpré-Girard[a], Richard Martel[a], Thomas Robert[a], René Lefebvre[a], Jean-Marc Lauzon[b]

[a] INRS-Eau, Terre et Environnement, Institut national de la recherche scientifique, Université du Québec, 440 Boul. de la Couronne, Québec, Québec, Canada, G1K 9A9

[b] TechnoRem Inc., 4701 Rue Louis B Mayer, Laval, Québec, Canada, H7P 6G5

DOI : 10.1016/j.jconhyd.2016.09.001

Résumé

Cette étude avait pour objectif d'évaluer le contrôle de mobilité d'une mousse faite à partir de solution tensioactive et son efficacité de récupération récupération d'un liquide immiscible léger (LIL) dans un milieu hétérogène. Le LIL était représenté par le p-xylène et un bac de sable a été utilisé pour représenter un milieu hétérogène. Des travaux similaires ont aussi effectué des essais d'injection en modèle 2D mais en utilisant d'autres détergents et leurs contaminants étaient des liquides immiscibles denses (LID). Dans le cadre de cette étude, le montage expérimental était constitué d'un bac 2D contenant deux couches de sables de silice de granulométries différentes, un sable moyen et un grossier. Le tensioactif utilisé est Ammonyx Lo (Stepan) à une concentration de 0.1% concentration de 0.1% dont l'efficacité pour la formation de mousse et la récupération de p-xylène a été démontrée lors de travaux antérieurs. Plusieurs essais en bac ont été effectués : des essais de traçage dans le bac non contaminé et contaminé, un essai d'injection de mousse dans le bac non contaminé ainsi qu'un essai de traitement avec de la mousse dans le bac contaminé au p-xylène. L'essai de traçage contaminé a permis l'observation d'une hausse du contraste de perméabilité entre les deux couches, indiquant que la contamination du bac influençait de façon plus marquée la couche moins perméable de sable ce qui augmente le contraste de perméabilité entre les deux couches. L'essai d'injection de mousse dans le bac non contaminé a démontré un meilleur contrôle de mobilité avec la formation d'un front ayant une forme de «S» alors que les essais de traçage avaient présenté des fronts en forme de pistons. Aussi, le balayage complet du bac a nécessité 1.8 volume des pores (VP) de solution liquide lors de l'injection de mousse et 2.8 VP pendant l'essai de traçage ce qui démontre une meilleure efficacité de balayage. Le pré-rinçage du bac avec la solution tensioactive a permis d'amorcer la mobilisation sans que de la phase libre soit

récupérée à l'effluent. Le traitement avec la mousse a permis d'atteindre une saturation résiduelle négligeable dans le bac. Cependant, le bilan de masse indiquait une récupération de seulement 48% de la masse initiale de p-xylène ce qui a mis en évidence une sous évaluation de la volatilisation. Lorsque la récupération grâce à la volatilisation a été corrigée, les taux de récupérations étaient les suivants : 19% de mobilisation, 16% de solubilisation et 65% de volatilisation. Ces résultats démontrent l'efficacité de l'injection de mousse pour le traitement de p-xylène dans un milieux poreux hétérogène. Des études complémentaires sont nécessaires afin d'optimiser le système par la production de mousse in situ afin de pouvoir l'appliquer à l'échelle du terrain.

Abstract

This study aimed to assess the ability of surfactant foam to achieve good mobility control and LNAPL recovery in a heterogeneous porous media. P-xylene was used as a LNAPL and a 2D sandbox to represent a heterogeneous porous media. The experimental setup consisted of a 2D sandbox filled with two layers of silica sand with different grain sizes: a coarse and a medium sand and the surfactant solution used was Ammonyx Lo at a concentration of 0.1% that was shown to have good foaming ability and the potential to recover p-xylene in a previous study. Tracer tests were done in both contaminated and uncontaminated sandbox, foam injection in the uncontaminated one and surfactant and foam injection in the contaminated one. The tracer tests indicated that the permeability contrast between both layers was increased by LNAPL contamination. Foam injection in the uncontaminated case presented a "S" shaped front which indicated a better mobility control than the piston shape front obtained during tracer tests. During foam injection, the complete sweep of the sandbox was achieved with 1.8 pore volume (PV) based on liquid recovery compared to 2.8 PV during tracer injection. Pre-flush of the contaminated sandbox with surfactant solution initiated p-xylene mobilization but no free phase was recovered at the effluent. A negligible residual saturation was reached following foam injection in the contaminated sandbox. However, mass balance indicated a total recovery of only 48% of the initial p-xylene, thus indicating an understimation of the recovery by volatilization. Corrected recovery values by volatilization were hypothesized and gave the following proportions: 19% by mobilization, 16% by dissolution and 65% by volatilization. These results show how efficient foam injection could be for the treatment of p-xylene in heterogeneous porous media. Follow-up studies should be done in order to improve the system via in situ foam production for a field scale application.

4.1 Introduction

4.1.1 Overview

In a context of enhanced NAPL recovery in shallow soils, the use of conventional in situ methods such as venting or bioslurping may be discouraged depending on site specific characteristics. In the case of a non volatile and viscous contaminant or when buildings are situated above the contamination, non conventional methods such as surfactant solution injection may constitute a better option. However, contacting the contaminant with the treating solution is a major issue when treating solutions are used. Preferential flow paths caused by fingering or by permeability contrasts can divert the solution and prevent its contact with part of the contamination. To avoid these problems, water-soluble polymers can be coupled with the surfactant solution in order to improve mobility (Martel et al., 1998, 2004; Robert et al., 2006). Polymers can enhance mobility control by their shear-thinning behavior and the increase of the washing solution viscosity (Lake, 1989). Foams can replace polymer as they also enhance mobility control with their shear-thinning properties and their large viscosity. Moreover, foam can enhance mobility control of the surfactant solution by lowering the relative permeability of the washing solution due to the presence of air (Hirasaki et al., 1989; Falls et al., 1989). Surfactant and polymers being expensive, another advantage of foams is that high proportions of air constitute each unit volume of foam (Rothmel, 1998), which can lower the needed amount of surfactant to remediate a site. Also, foam can be made with very low concentrations of surfactant.

Our study was done in the context of the application of foam to remediate LNAPL-contaminated soils by p-xylene. Our general objective was to better understand the processes related to foam remediation, especially the flow of foam in layered soils with contrasts in hydraulic properties. The steps followed in the study were: 1) the design and the evaluation of the flow properties of a 2D sandbox filled with two grain sizes sands, 2) the testing of foam injection in this sandbox to evaluate foam behavior in layered porous media and 3) remediation of the sandbox, after contamination with p-xylene, using surfactant and foam injection. This laboratory study aimed to provide a basis to assess the feasibility of such an application of foam for the remediation of LNAPL-contaminated shallow soils.

This work represents the second step of a project leading to field-scale testing of foam for LNAPL remediation. The first step involved surfactant selection and 1D column testing (Longpré-Girard et al., in prep.).

All tests used homogeneous clean sand, distilled water, a single surfactant solution at a time (no mixtures) and contaminated tests used pure p-xylene dyed with Oil-Red-O for visual observation. Since this work is carried out in the context of an eventual field application, practical considerations imposed the following constraints on the approach: 1) use a low surfactant concentration to lower costs; 2) use a low injection pressure to prevent soil heaving; and 3) aim for the creation of a stable foam front to avoid fingering and loss of NAPL during NAPL recovery.

4.2 Theory

4.2.1 NAPL enhanced recovery mechanisms with surfactants and foams

Three recovery mechanisms can take place during foam treatment: mobilization, dissolution and volatilization. In the context of foam injection for the treatment of LNAPL-contaminated soil, the main mechanism should be mobilization in order to recover more mass for the pore volumes of foam injected in the soil. Dissolution and volatilization still take place but no attention was put into optimizing these processes.

NAPL can be mobilized via the increase of the capillary number (N_c), which is the ratio of viscous over capillary forces, defined as follows:

$$N_C = \frac{q\mu}{\sigma cos\theta_v} \qquad \textbf{Equation 4.1}$$

Where, q is fluid flux (m/s), μ is fluid viscosity (Pa·s), σ is interfacial tension (mN/m) and θ is the contact angle (°) representing the effect of wettability. N_c values between $1x10^{-5}$ and $5x10^{-5}$ were considered by Pennell et al. (1996) as needed for the initiation of PCE mobilization in contaminated silica sand columns and a value of $1x10^{-3}$ was needed for complete displacement. The increase in viscous forces is achieved by the increase of the injected fluid viscosity and its velocity in the porous media whereas the decrease in capillary forces is possible via the interfacial tension reduction by surfactant. Therefore, maximizing N_c favors the possibilities of contaminant displacement by foam. So, each step of this study was made in order to maximize N_c on every possible level. Replacing water by foam in porous media favors NAPL mobilization

because it increases viscosity and decreases interfacial tension by at least one order of magnitude. In the first part of this project (Longpré-Girard et al., in prep.), interfacial tensions and foamability were measured for several surfactants and the best candidate with the lowest interfacial tension with the contaminant and the best foamability was selected for 2D sandbox tests carried out in the second part of the project whose results are presented in this paper.

The solubility of NAPL in the liquid phase of foam is increased by surfactant with a concentration above its critical micelle concentration (CMC). The amount of NAPL solubilized is given by the Chun-Huh equation (Pope and Bavière, 1991):

$$\sigma = {}^{c}/_{R^2} \qquad \textbf{Equation 4.2}$$

where, c is typically equal to 0.3, and R is the dissolution ratio relating the volume of NAPL solubilized in the micellar phase to the volume of surfactant.

Volatilization of the NAPL by foam injection is occurring because foam is a mixture of liquid and air. P-xylene being volatile, volatilization may enhance its recovery in a significant way. P-xylene is the only compound dissolved in water so its volatilization can be evaluated considering its vapor pressure (P_v) and the Ideal Gas Law, which is defined as follows:

$$P_v V = nRT \qquad \textbf{Equation 4.3}$$

Where V is volume (m³), n is the number of moles, R is the ideal gas constant (8.31 J/Kmol) and T is temperature (°K).

4.2.2 Mobility control with polymers and foams

A major challenge in enhanced NAPL recovery in contaminated soil is to uniformly sweep the contaminated zone and contact every pocket of contaminated soil present in the treated zone. Many methods have been developed to distribute treatment fluids, such as liquid surfactants, in heterogeneous soils with permeability contrasts, and two of them are polymers and foams. Both of these methods increase mobility control by an increase in viscosity, which slows down the movement of injected fluids in the higher permeability zones, so that flow also occurs in the lower permeability zones because of a shear thinning behavior. In fact, both foam and polymer have non-Newtonian and shear-thinning properties, which means that when shear stress increases, viscosity decreases, as in low permeability porous media creating a stable front in heterogeneous media. Polymers behavior in porous media was extensively studied for their

mobility control properties in porous media (e.g. Martel, 1995; Martel et al., 1998; Martel et al., 2004; Silva et al., 2012; Robert et al., 2006).

Foam injection enhances mobility control in two distinct ways (Falls et al. 1989): by decreasing water relative permeability with the presence of air and by increasing the apparent viscosity. Hirasaki and Lawson (1985) studied the behavior of foam bubbles in smooth capillaries and found that foam increases viscosity because of the shear force between the gas liquid interface and the pore walls, which slows the advance of the bubble. Moreover, Falls et al. (1988) found that viscosity was not only enhanced by shear stress but was also increased by the force required to push lamellae through constricted pore throats when flowing through porous media.

4.3 Methodology

4.3.1 2D Sandbox experimental setup

A short list of materials can be put in contact with p-xylene without having a reaction; glass, stainless steel, Teflon and nylon. That is the reason why those materials were the only ones used for the sandbox setup knowing that tests would be carried out with p-xylene-contaminated soil.

The sandbox design was based on Martel et al. (1995). Because of the injection pressures that were used, possible deformation and leakage of the sandbox had to be considered during its design. For this reason, the number of moving parts and potential leaking joints were minimized in order to reduce possible leakage of injected fluids. Also, thick walls were used to reduce possibilities of deformation due to high injection pressure. The sandbox consists of a stainless steel box (1.5 cm thick walls) opened on top with an internal volume of 2.5 L and a tempered glass window (1.5 cm thick) on the front side that allows visualization of all experiments (Figure 4.1). Pictures of every test were taken with a digital camera (Nikon, Coolpix P510), which allowed the analysis of test results. The sandbox is closed on top by a 2.1 cm thick nylon plate overlaid with a 0.65 cm stainless steel plate to minimize deformation.

A distribution chamber, allowing fluid injection or recovery, was placed at each end of the sandbox as shown in Figure 4.2 (b). Both chambers were made of nylon: a perforated plate was placed over a reservoir of 10 cm by 5 cm and 1 cm deep with a threaded opening on top in which a quick-connect connector was screwed. This setup allows fluids to be distributed uniformly before they enter or leave the sandbox, as shown in Figure 4.2 (a). A stainless steel

screen with 250 µm openings was placed over each chamber to prevent the loss of fines. Clay (crafting quality, Vallauris) was placed around both chambers to seal gaps between the sides of distribution chambers and the sandbox walls. As shown in Figure 4.1 (b), threaded holes were made through the sandbox back at equal distances in order to connect pressure transducers. Stainless steel mesh was placed over each hole in order to prevent sand leaking. Four pressure transducers were disposed throughout the system to measure changes in pressure along the system as shown in Figure 4.2 (b); one at the sandbox inlet (T-1), one at the first two pressure ports of the upper layer (T-2 and T-3) and one in the first pressure port of the lower layer (T-4). The pressure transducers (GP-50 model 311, InterTechnology) were linked to electronic data loggers (ES-120, Dickson) and their electric signal was then converted to pressure values with DicksonWare 9.0.8 software.

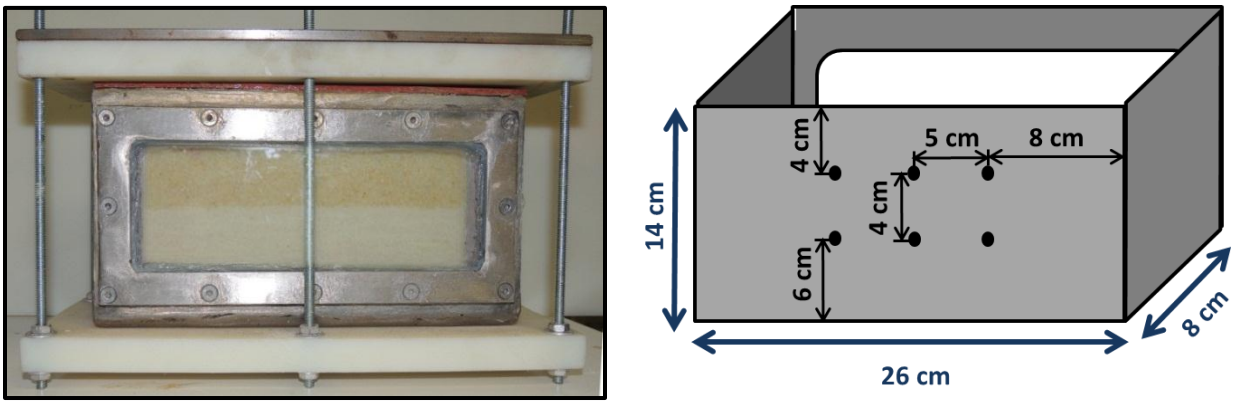

(a) (b)

Figure 4.1 – (a) Photo showing a general view of the sandbox setup. (b) Schematized back view of empty stainless steel sandbox with glass window in background.

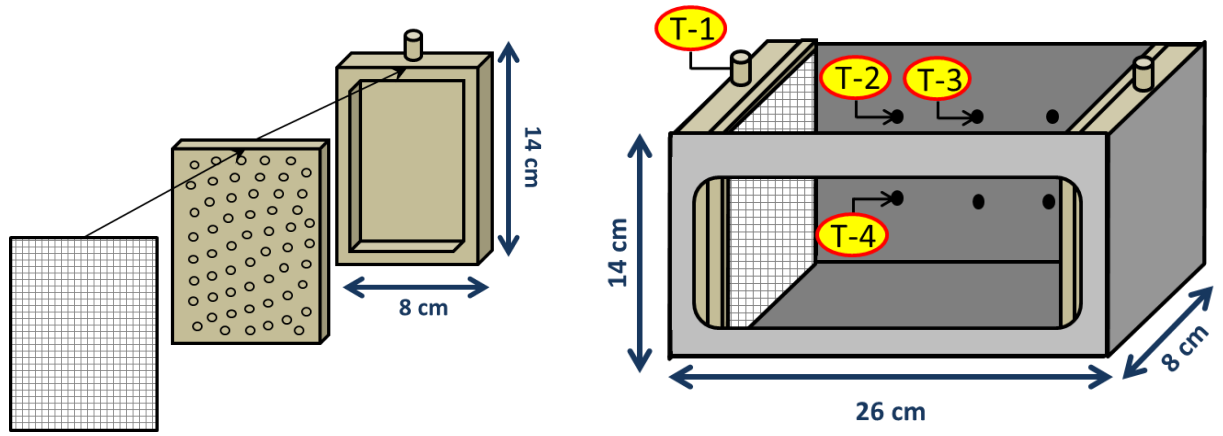

(a) (b)

Figure 4.2 – (a) Schematized nylon distribution chamber details; distribution chamber closed by a perforated plate overlaid by a stainless steel mesh screen. (b) Schematized empty sandbox with distribution chambers shown. T-1 through T-4 refer to pressure transducers.

Because of initial problems in the sandbox design, a small gap of 2.1 cm at the bottom of each distribution chamber was not covered by the perforated plate. Therefore, a nylon plate with a 2 cm thickness was placed on the sandbox bottom, which prevented any fluid flow in this part of the sandbox. Clay was disposed on this plate and scarified to minimize preferential flow paths between the plate and the layer of sand overlaying it. The same setup was installed at the upper end of the sandbox for the same reasons but the gap was filled with a 0.72 cm thick nylon plate with clay underneath. That way, no fluid flow dead zone could form as all the cross section of sand was in hydraulic contact with both distribution chambers at the entry and exit of the sandbox.

The glass window in front of the sandbox did not show the entire width of the sand. Two layers of sand with different grain sizes were placed in the sandbox. The interface between the two sand grain sizes was placed to appear in the middle of the window but the presence of the nylon plate at the bottom shifted its position. Therefore, the coarser sand layer on top had a slightly greater thickness than the finer sand layer at the bottom.

Silica sand (99.9% quartz) was used for all experiments in order to minimize fines (clay and silt) and organic matter contents and the interaction of surfactant and contaminant with them and other minerals. Two grain sizes of silica sand were used (Table 4.1); Temisca 20 (Opta Minerals Inc.), a coarse sand and Flint (Bell & Mackenzie, Hamilton) a medium sand. A hydraulic conductivity ratio of 2.71 between both sands can be evaluated with the sand properties indicated in Table 4.1.

Table 4.1 – Properties of silica sands used for sandbox tests, d_{10} and d_{50} refer to grain sizes larger than 10% and 50%, respectively, of sand mass.

	D_{10}	D_{50}	Hydraulic conductivity (K) (m/s)
Temisca 20	0.75 mm	1.3 mm	3.2×10^{-4}
Flint	0.43 mm	0.53 mm	1.2×10^{-4}

The horizontal effective hydraulic conductivity (K_e) of the system can be calculated by the arithmetic average of each layer conductivity (K_i) with its thickness (h_i) (Freeze and Cherry, 1979):

$$K_e = \frac{\sum K_i h_i}{\sum h_i} \qquad \textbf{Equation 4.4}$$

The filling and compaction of columns were done as described by Martel and Gélinas (1996). The compaction of every 4 mm layer was made by dropping a 293 g weight from a height of 19

cm until a global dry density of 1.7 g/cm³ was attained to prevent channeling (Ripple et al., 1973). Each layer was scarified after its compaction to minimize preferential flow between each layer.

When the sandbox filling was completed, the top was closed with a 0.35 cm thick rubber sheet overlaid by a 2.1 cm thick nylon plate and a 0.65 cm thick stainless steel plate to prevent deformation. Another nylon plate was placed underneath the sandbox aligned with the overlaying plate. Then, the sandbox was squeezed between both nylon plates with 6 endless screws and rivets. Sealing was assured by a layer of waterproof silicon laid over every joint of the setup.

4.3.2 Water and p-xylene saturation

When silicon had dried and all tubing connections were made, the sandbox was purged with pressurized CO_2. Then, water saturation was established by placing the sandbox on its short side and filling it from bottom up with deoxygenated deionized water. A total pore volume of 543 ml corresponding to a porosity of 0.35 was measured by weighting the sandbox dry and saturated with water.

Contamination of the sand was done by downward injection of p-xylene dyed with 0.9 g/L of Oil-Red-O (Sigma-Aldrich) in the saturated sandbox while placed on its short side. Unfortunately, after three minutes of injection, the coarse sand layer was completely swept while only a small portion of the medium sand layer had been swept as shown in Figure 4.3.

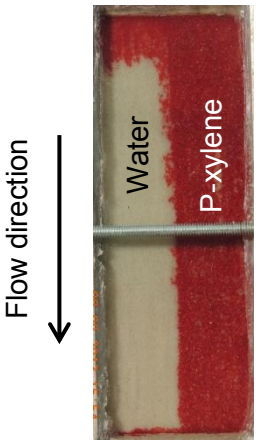

Figure 4.3 – Photo of the distribution of contaminant in sandbox after the first saturation with p-xylene.

A test was then made to attempt to sweep the fine sand layer by putting the sandbox upside-down and injecting liquid from the pressure port on the top right-handed side of the sandbox as shown in Figure 4.4. This method seemed to form preferential paths for p-xylene, and Figure 4.4 (a) shows the final contamination achieved with this method.

The last and best technique to sweep the finer sand with p-xylene was to extract liquid from the pressure ports placed on the sandbox back while the injection ports were dipping in p-xylene and the sandbox was still upside down. This setup assured that the only fluid entering the system was p-xylene and the upside down position improved p-xylene movements because of the density contrast with water. Figure 4.4 shows the p-xylene saturation progression of Flint layer through time using this method. P-xylene was pumped in closed circuit for about 15 hours in total. The region in the upper right part of the sandbox on Figure 4.4 was not completely swept by p-xylene because it is the portion that was used to test the injection of p-xylene by the pressure port which created preferential flow paths that prevented the sweep of the region by p-xylene.

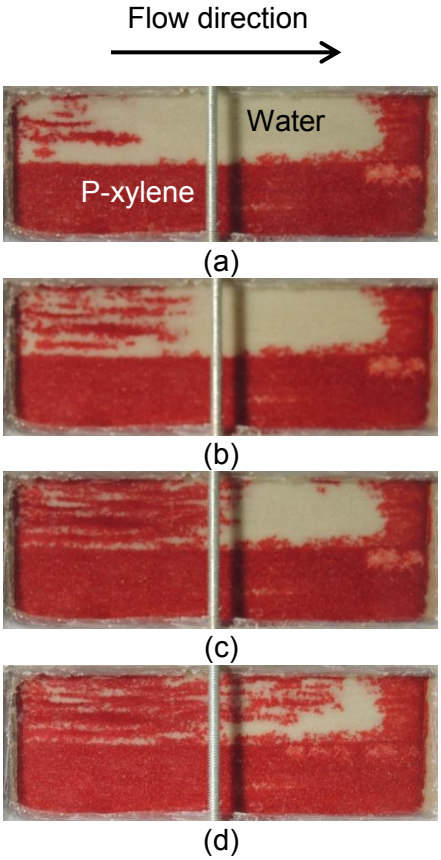

Figure 4.4 – Photos of contaminant saturation of Flint layer in sandbox through time achieved by pumping in pressure ports while sandbox is upside down (a) initially, and after (b) 3h30, (c) 5h30 and (d) 15h00.

After contamination, the sandbox was placed on its short side and rinsed from bottom up with distilled water to bring it to residual oil saturation (S_{or}). Water breakthrough happened at 3 minutes 28 seconds, which fits with the complete sweep of Temisca 20 layer as shown in Figure 4.5 (c). A total of 14 L of water was injected over a 2h40 period and a p-xylene residual saturation of 90 ml was left in the sandbox, which corresponds to a saturation of about 17% of the total porosity bringing the contaminated effective pore volume to 453 ml corresponding to a porosity of 0.29.

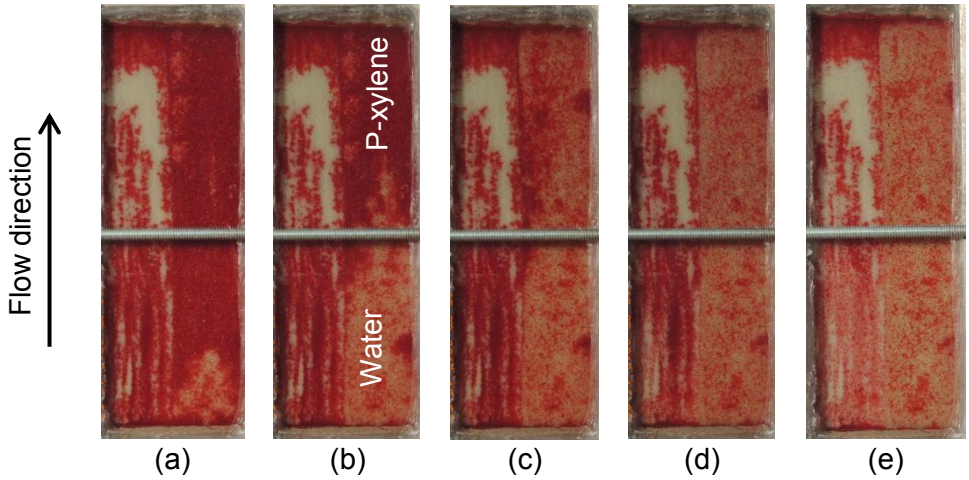

Figure 4.5 – Photos of p-xylene saturated sandbox placed on its short side and rinsed from bottom to top with water to bring it to residual oil saturation, after (a) 9 ml, (b) 20 ml, (c) 70 ml, (d) 150 ml and (e) 14 L of water injection.

4.3.3 Tracer tests

Tracer solution was injected at a constant flow rate of 14 mL/min with a peristaltic pump (model 7553-70, Cole Parmer). Two tracers were used in the same solution; amaranth (Sigma-Aldrich) as a visual tracer and potassium bromide (Laboratoire Mat) as a conductive tracer. Both tracers do not adsorb on silica sand and no interactions were observed between them. Samples of 40 mL were taken at the outlet for all test duration. Bromide ion concentration was measured with a bromide electrode (Orion model, Thermo Scientific).

For the contaminated tracer test, two tracers were used; bromide and a blue food coloring. Amaranth could not be used because of the already red coloring of p-xylene with Oil-Red-O making the visual tracking of amaranth impossible. Food coloring was used only for the purpose of visually tracking tracer progression during the experiment because it is adsorbed on silica sand. Therefore, there is a delay between food coloring progression and bromide progression through the sandbox. Injection rate was fixed at 13.75 mL/min.

4.3.4 Foam injection

The foam injection system used for sandbox experiments was the same as the one developed and applied for sand column tests (Longpré-Girard et al., in prep.; Section 3.2.2). After the tracer test, a foam test was also carried out. The surfactant used was Ammonyx Lo from Stepan at a concentration of 0.1% w/w. As in column tests, the foam production column was purged with foam until foam quality was stable then the foam production column outlet was connected to the sandbox inlet. The sandbox was saturated with water prior to foam injection. Injection pressure was increased throughout the experiment in order to maintain the foam front advance.

Treatment of the contaminated sandbox was done in two steps: 1) injection of liquid surfactant solution and; 2) foam injection. Previous column tests indicated that a pre-flush with surfactant solution having the same concentration as foam prior to foam injection facilitated the formation of a clear stable foam front. For this reason, 1 L of liquid surfactant was injected in the contaminated sandbox prior to foam treatment. A peristaltic pump was used for the injection of surfactant solution at a constant flow rate of 14 mL/min. This pre-flush is comparable to a liquid surfactant treatment, so it was interpreted as such. After liquid surfactant injection, foam was injected in the contaminated sandbox. Injection pressure was increased throughout the experiment in order for the front to keep advancing, as the presence of viscous foam in the sandbox renders flow more difficult. The effluent was recovered and free LNAPL phase recovery was followed through time. Discrete liquid samples were taken to estimate dissolved p-xylene concentrations. Also, air was sampled at the sandbox outlet to assess volatilized organic pompounds (VOC) concentrations. For the purpose of air sampling, the output tubing was placed in the opening of a Mason jar without touching the liquid that was accumulating at the bottom of the jar. A parafilm paper was then placed over the jar opening in order to seal it as best as possible. Air samples were taken by piercing a small hole in the parafilm paper with a needle and sampling the air over the liquid. VOC concentration was measured with a Portable gas chromatograph (GC Voyager, Photovac). Air flow was estimated by the travel speed of foam lamellae between two marks on the outlet transparent tubing. Knowing the volume contained in the tubing between these two marks, air flow could be estimated when travel speed was low. Overnight pauses were made during foam injection because of the length of the test. The inlet of the sandbox was closed to stop foam injection, the outlet was kept open to release some of the pressure. Then, the outlet was also shut to prevent leakage. When foam injection was resumed, the same injection pressure was used as when the test was stopped.

4.3.5 Sampling and analytical methods

To limit the time needed to complete the experimental program, all tests described below were carried out on the same sandbox filled with sand only a single time. Therefore, the sandbox was rinsed between each test; using water after the tracer test or with water and dried with air and CO_2 and then rinsed again with water after a foam test. Following that logic, the contaminated test was the last test carried out before opening and sampling of the sandbox. Samples of the treated sandbox could only be taken about 3 weeks after the end of foam injection. Even at the end of foam treatment, some regions of the sandbox remained strongly contaminated according to their color. Therefore, both layers of sand were sampled in three different regions: 1) clean zones, 2) slightly contaminated zones and 3) strongly contaminated zones. In each zone, at least a grab sample and a composite sample were taken. A total of 16 subsamples of 5 g were taken, put in 10 ml of methanol to dissolve p-xylene and analyzed with gas chromatography mass spectrography (GC/MS). Method EPA 8260B was used with a PerkinElmer Turbomatrix Headspace 40 trap connected by an inert heated transfer line to a PerkinElmer Clarus 500 GC-MS. Analyzes were done using a DB-5MS UI 30 m x 0.25-mm i.d. and a 0.25-μm film thickness. Results were converted in mg of contaminant per kg of dry soil. Then, each sand zone was isolated in an open container and left to dry to measure its dry weight. With those measurements, it was then possible to convert each zone having distinct contaminant concentrations, based on dye color intensity, into contaminant weight and then quantify the total mass of p-xylene remaining in the sandbox.

4.4 Results and discussion

4.4.1 Overall Conductivity and Porosity

A total pore volume of 543 ml, corresponding to a global porosity (n) of 0.35 was measured by weighting the sandbox dry and then saturated with water. Also, pore volume was calculated using sand volumes and weights measured during the sandbox filling. With these measurements and knowing that silica has a density of 2,650 kg/m³, the volume of solids (V_S) and the pore volume (PV) were calculated for each sand layer. Results are presented in Table 4.2. The global pore volume of 548 ml calculated with this method is consistent with the global pore volume of 543 ml measured by weighting the sandbox dry and saturated, the 5 ml difference between these estimates being negligible.

Table 4.2 – Total pore volume in the sandbox based on measurements made during sandbox filling and by weighting the sandbox dry and saturated (ml)

Sand type	Total pore volume (ml) based on two methods		Estimated porosity
	Sandbox filling measurements	Saturated and dry weight	
Temisca 20	329	n.m.	0.37
Flint	219	n.m.	0.33
Global	548	543	0.35

n.m.: not measured.

A permeability contrast of 2.71 was evaluated with sand properties as indicated in Table 4.1. Also, an effective hydraulic conductivity of 2.8×10^{-4} m/s was evaluated with Equation 4.4 for the entire sandbox.

4.4.2 Tracer tests

In order to determine the effective ratio of hydraulic conductivities in the sandbox, a tracer test was carried out. Observation of Figure 4.6 indicate a piston-shaped front in each layer with a significant delay between them, the visual tracer swept the coarser sand first and then swept the finer sand. Temisca 20 sand was completely swept by amaranth after only 31 minutes, as shown in Figure 4.6 (b) which is about 0.25 of the total injection time of 2 hours 8 minutes needed for the whole sandbox to be swept. Bromide full concentration at the output was attained after 1550 mL of injected solution (2.8 PV), after about 1 hour 55 minutes, so there is a delay of 13 minutes between the full sweep of the visual tracer and bromide tracer full concentration at the output, which can be due to a light sorption of amaranth.

The fronts for the tracer test carried out in the p-xylene contaminated sandbox show similar behavior as those for the uncontaminated tracer tests; i.e. a piston-shaped front with a clear delay between the fronts in the two sand layers. Besides the shape of the front, no reliable information can be taken from Figure 4.7 because of the delay of the colored front with the bromide front due to dye adsorption.

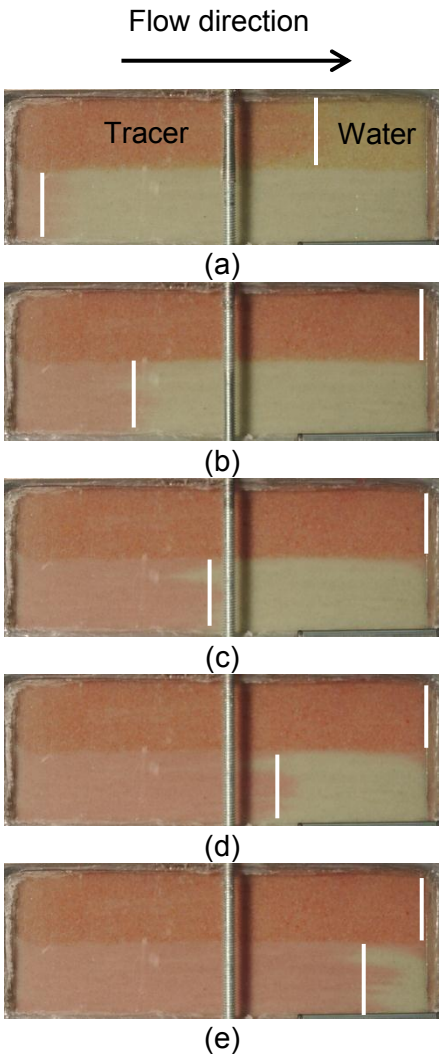

Figure 4.6 – Photos of tracer test in the uncontaminated sandbox, white lines indicate the position of the tracer front after (a) 0.5 PV, (b) 1 PV, (c) 1.5 PV, (d) 2 PV and (e) 2.75 PV (PV is based on the total pore volume in the entire sandbox).

Study of the arrival curves shown in Figure 4.8 indicates a gap between the uncontaminated and contaminated arrival curves caused by the presence of residual p-xylene in some of the pore volume. For the uncontaminated tracer test, the injection of 2.75 PV was needed to attain full concentration at the output, 2.86 PV were needed for the contaminated test. Also, both curves have a bimodal shape caused by the presence of the permeability contrast between the coarse and medium sand layers. This curve shape prevents the use of standard tracer test analytical solutions, such as Ogata-Banks (Ogata, 1970), for the interpretation of results. However, front velocity and permeability contrast were evaluated according to bromide arrival curves at the outlet with simple calculations. First, the two plateau concentrations had to be identified for each test. Then, knowing that the only bromide concentration flowing at the outlet

came from the coarse sand layer and was diluted by the water exiting from the medium sand layer, a global mass flux was evaluated to calculate the flow rate of the coarse sand layer. With these values, flow rate in each layer was evaluated. Then, using Darcy's Law, a permeability ratio of 2.99 was evaluated between the two sand layers for the uncontaminated test and a ratio of 5.9 was evaluated for the contaminated test (Table 4.3). The increase in permeability ratio due to the contamination of the sandbox implies distinct effect of contamination on the two sand layers. Contamination reduced permeability in the medium sand layer more than in the coarse sand layer. This is shown by the wider gap between the two arrival curves after the first plateau compared to the gap before the first plateau (Figure 4.8).

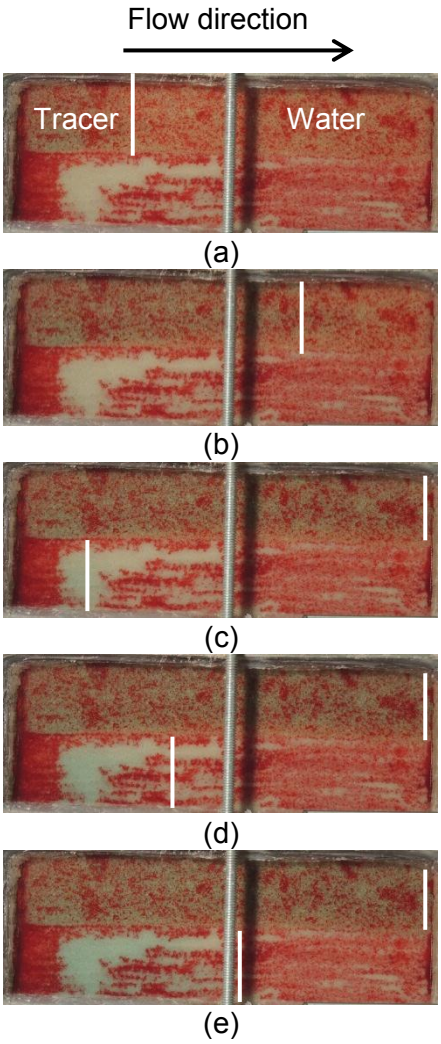

Figure 4.7 – Photos of the tracer test carried out in the contaminated sandbox, the white lines indicate the position of the tracer front after (a) 0.5 PV, (b) 1 PV, (c) 1.5 PV, (d) 2 PV and (e) 2.9 PV (1PV is 453 ml).

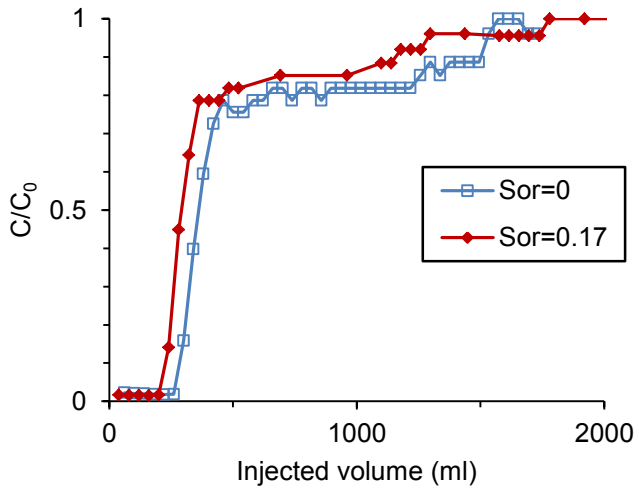

Figure 4.8 – Uncontaminated and contaminated sandbox bromide tracer arrival curves.

A "U" shaped water manometer was used to measure the pressure gradient during tracer injection in the contaminated sandbox. So, a global effective permeability of 1.97×10^{-11} m² for the whole sandbox was evaluated according to Darcy's Law. A summary of conductivities and permeability contrasts are presented in Table 4.3. Permeability contrasts calculated with the theoretical values and with tracer test measurements in the uncontaminated sandbox are consistent with values of 2.71 and 2.99 respectively. Considering the larger permeability contrast between the two sand layers after p-xylene contamination, creating a favorable mobility control with foam injection became even more important in order to fully sweep the entire sandbox.

Table 4.3 – Effective permeability contrasts.

	Theoretical	Tracer S_{or}=0	Tracer S_{or}=0.17
Effective Permeability (m²)	2.35×10^{-11}	NM*	1.97×10^{-11}
Permeability Ratio between Sand Layers	2.71	2.99	5.9

* NM: Not measured.

4.4.3 Uncontaminated foam test

As mentioned before, injection pressure was increased throughout the foam test from 150 cm H_2O to 525 cm H_2O (14.7 kPa to 51.5 kPa) in order to keep the foam front advancing. The test lasted 3 hours 30 minutes and about 1 L (1.8 PV) of liquid surfactant was used. Compared to the tracer test with water (Figure 4.6), Figure 4.9 indicates that foam injection created a more

uniform front advancing at the same velocity in both sand layers. This is a major improvement in sweep efficiency when compared with water and tracer injection in Figure 4.6 where two clear piston-like fronts advanced with a significant delay between them. So, better mobility control is achieved by foam injection, creating a more uniform front between both layers. However, as previously observed during foam injection in column tests, 2 foam fronts can be observed on Figure 4.9: a first foam front with poor sweep efficiency (yellow solid line) and a second front with better sweep efficiency (red dotted curve). The first front presents some fingering but advances at the same velocity in both layers. The second foam front has a clear "S" shape. Air started exiting the sandbox after 2 minutes 50 seconds of foam injection, thus indicating a preferential air flow path probably located in the upper part of the sandbox.

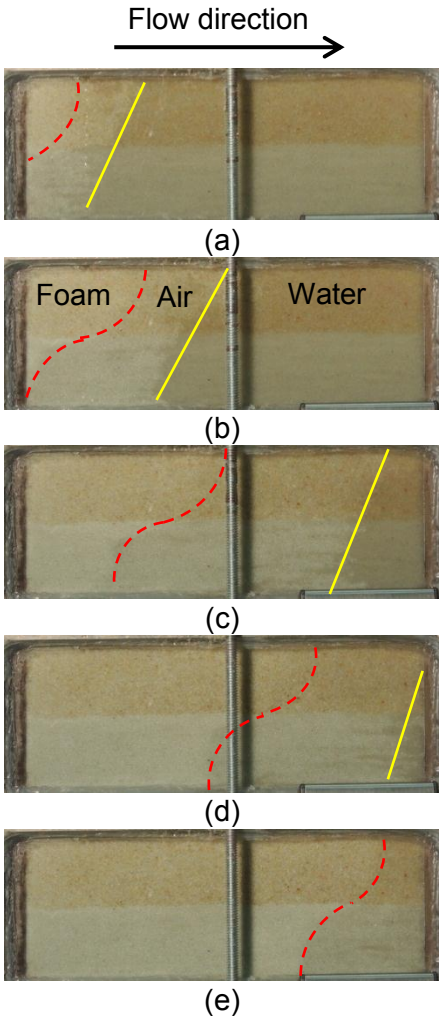

Figure 4.9 – Photos of foam injection experiment in uncontaminated sandbox after (a) 1 min, (b) 5 min, (c) 29 min, (d) 59 min and (e) 2 hours 5 min.

4.4.4 LNAPL remediation

Surfactant pre-flush of the contaminant sandbox is comparable to a liquid surfactant treatment. Therefore, a capillary number of $3.42x10^{-5}$ can be estimated with Equation 4.1. This value fits in the range of $2x10^{-5}$ to $5X10^{-5}$ evaluated by Pennell at al. (1996) to be needed to initiate mobilization of PCE in silica sand. However, a negligible mass of p-xylene was recovered during surfactant injection. In Figure 4.10 (d), the dotted black ellipse highlights a zone of contaminant moving towards the sandbox upper part, which indicates a mobilization of the contaminant and an upward movement caused by density contrast. Trapping of p-xylene in the upper part of the sandbox caused by design problems may explain the negligible recovery of p-xylene free phase during liquid surfactant injection, even though some mobilization occurred.

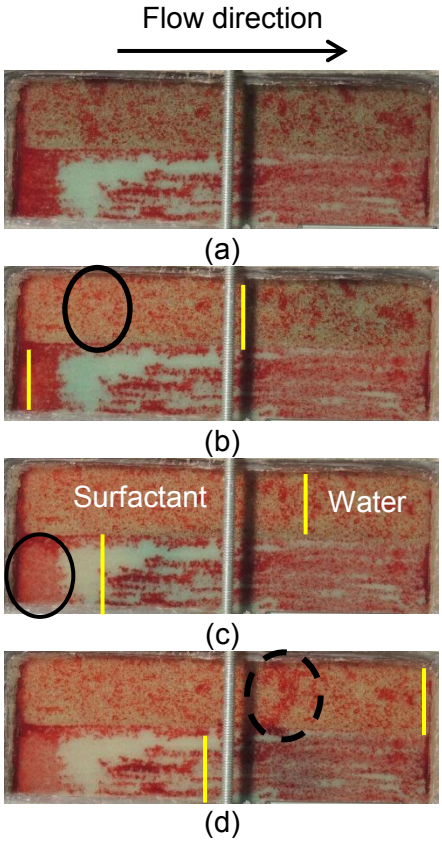

Figure 4.10 - Photos of contaminated sandbox pre-flushed with liquid surfactant prior to foam treatment, (a) initially and after (b) 0.55 PV, (c) 1.1 PV and (d) 2.2 PV. (1 PV is 453 ml)

The tracer test with a bromide solution was done prior to surfactant injection. Both injections, with and without surfactant, had similar flow rates and both solutions had the same viscosity. The only difference between both tests was the lowering of interfacial tension going from 23.87 mN/m during tracer test to 0.79 mN/m during surfactant injection. The black ellipses on Figure

4.10 (b) and (c) highlight regions that were partially cleaned by surfactant injection. There is still contamination left, as red coloring is present after the passing of liquid surfactant front, but the faded red color indicates a lowering of p-xylene concentration at these locations.

Foam injection followed surfactant solution flushing. Figure 4.11 gives a general idea of the efficiency of foam treatment of the sandbox contaminated with p-xylene. The complete removal of p-xylene from the regions swept by foam is obvious just by the change in color. Soil samples confirmed this, as p-xylene concentrations were below the detection limit of 16.3 mg/kg of dry sand. The detection limit is below the maximum concentration cirteria of 50 mg/kg for xylenes in soils for commercial and industrial sites in Québec, Canada (MEQ, 1998).

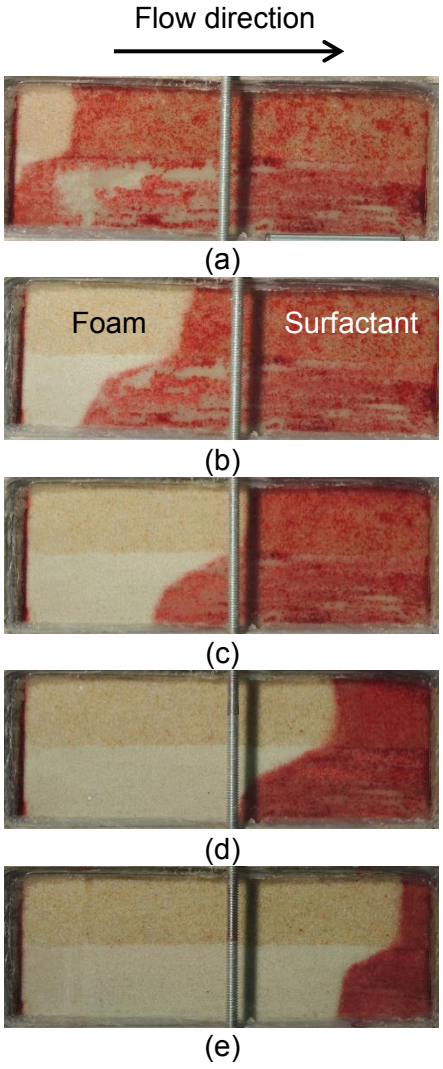

Figure 4.11 – Photos of foam treatment of contaminated sandbox (a) 34 min (b) 2h 30 min (c) 12 h (d) 26 h (e) 46 h.

A total of 15 L of surfactant solution were needed to bring the foam front to the position shown in Figure 4.11 (e), whereas 1 L was needed in the uncontaminated test to sweep the entire sandbox with foam. This difference may be explained by the foam collapse at the front when in contact with p-xylene, causing the separation of air and surfactant solution. The air rised and caused the air slugs observed at the effluent and the surfactant solution flowed ahead of the foam front. This surfactant solution went through successive mixings with p-xylene which caused a phenomena similar to multiple contact miscibility which is used in EOR to generate a miscible displacement of the oil phase. Successive mixing of the oil phase with the treating solution develop the miscibility as a consequence of the enrichment of the liquid phase with intermediate components (Lake, 1989). So, the successive contacts between the surfactant solution and p-xylene could have caused an induced miscibility of p-xylene that accumulated ahead of the foam front and generated the darkened red coloring as shown in Figure 4.11.

Based on free-phase recovery and concentrations measured in the liquid and gas phases, it was possible to assess the p-xylene mass in the effluent that was mobilized (free phase), dissolved (aqueous phase) or volatilized (gas phase). Figure 4.12 shows the recovery achieved by each mechanism individually and combined. Volatilization started gradually whereas dissolution was constant throughout the experiment and mobilization was achieved by steps. The mobilization of 3.4 g of p-xylene that occurred at the beginning of treatment was due to mobilization during surfactant injection that was not recovered prior to foam injection. The steps that shape mobilization recovery are the results of the sampling method which consists of filling 1 L containers and decanting it to measure the free-phase that was mobilized during sampling so, large quantities of free-phase were recovered. P-xylene concentration in air was first measured after 4.4 PV of liquid phase had exited the sandbox. Therefore, an extrapolation of the first results was extended to the period before 4.4 PV. Volatilization attained a plateau at the end of injection because of the lowering of p-xylene concentration in the sandbox. Dissolution was evaluated following p-xylene concentration measured in samples of the effluent. A mean concentration of 614 mg/L was measured and applied to the effluent volume to determine recovery through time. Therefore, the recovery by dissolution was conservative considering fluctuations in concentration at the effluent were not considered for the mass balance.

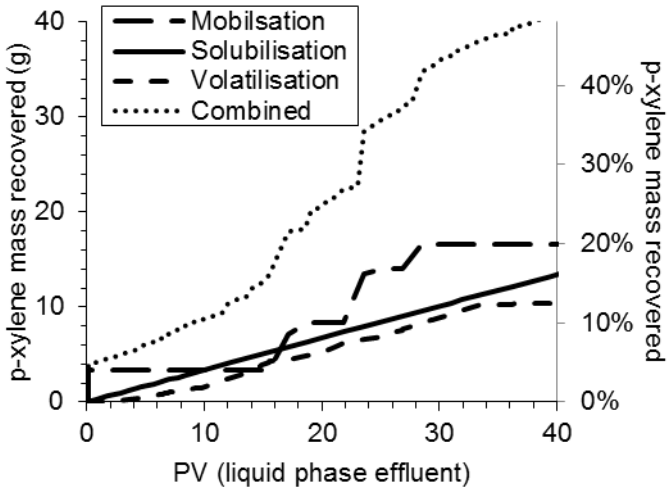

Figure 4.12 – P-xylene recovery with each mechanism and combined. PV is 548 ml.

Table 4.4 gives an overview of the recovery achieved by each remediation mechanism. With 19% of the removal, mobilization is the most efficient mechanism. However, the total of mass recovered by all mechanisms only represents 48% of the initial p-xylene mass in the sandbox. This is not coherent with sand samples at the end of the test, which indicated a remaining mass of only 0.263 g (0.29% of initial contamination). There is thus a gap of 51% (44 g of p-xylene) of the initial contamination between estimated mass recovery and remaining concentration in the sandbox. Recovery by mobilization and dissolution were evaluated with precise analytical methods having only small uncertainties. However, some technical problems caused a large uncertainty on the mass recovered by volatilization. Air volume could be evaluated only when air velocity in the output tubing was slow enough for the bubbles to be seen and their speed measured. Therefore, when the test was restarted after an overnight stop, for example, air flow rate was very rapid and could not be measured until it had slowed down. Air volume exiting the system was thus underestimated, which caused a large gap in mass balance. Table 4.4 indicates an estimation of volatilization recovery that closes the mass balance. In order to attain such volatilization, a total volume of 0.85 m³ at atmospheric pressure and a mean air flow rate of 241 mL/min at atmospheric pressure would have exited the setup for all the test length. Considering that the air flow was not constant throughout the experiment and air exited the setup as air slugs, this mean air flow rate is realistic and provides a confirmation that 0.85 m³ is a valid total air volume. In the context of future experimentations with foam treatment, a better air flow measurement system would be necessary.

Table 4.4 – Foam injection removal for each remediation mechanism and hypothesized recovery with corrected volatilization.

	Evaluated		Hypothesized	
	Removal (g)	Removal (%)	Removal (g)	Removal (%)
Mobilization	17	19	17	19
Dissolution	14	16	14	16
Volatilization	10	12	54	65
Total	41	47	85	100

Foam injection had to be stopped overnight because of the length of the test. These stops allowed observation of density contrasts as shown in Figure 4.13.

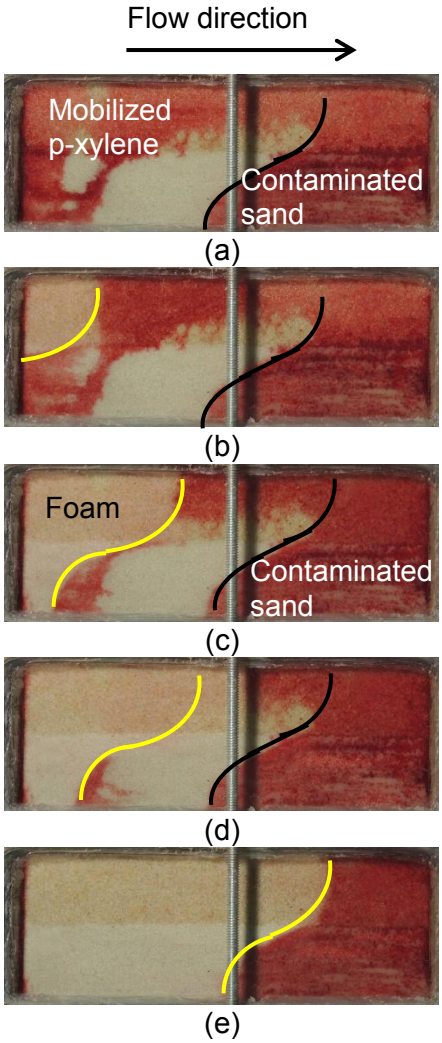

Figure 4.13 – Photos of foam injection in the contaminated sandbox after an overnight stop. The black line is the position of the front before the overnight pause, the yellow line is the foam front actual position. Photos show (a) initial conditions after the overnight stop and (b) 1 min, (c) 5 min, (d) 15 min and (e) 55 min after foam injection had resumed.

When the injection was stopped, the sandbox inlet and outlet were closed to minimize volatilization. Pressure then homogenized in the sandbox, foam collapsed and fluids redistributed themselves based on their relative densities: surfactant solution accumulated at the base of the sandbox, p-xylene placed itself over liquid surfactant and air occupied the upper part of the sandbox. Structures as shown in Figure 4.13 (a) were then formed. When foam injection was initiated again after the overnight stop, a foam front would form again with its typical “S” shape and push back the p-xylene that had moved downward during the injection discontinuation until it had taken its place back where it was the day before.

After all these tests, a sandbox test was done with an inverted configuration of sand to confirm some assumptions. In this sandbox, the coarse Temisca 20 sand was underlying the finer Flint sand. A water tracer test was carried out in this configuration without contamination. The white ellipse on Figure 4.14 (a) highlights an air bypass that occurred in the upper part of the Temisca 20 layer. This bypass could explain why, in foam tests, air always exited the sandbox before the foam front attained the output. However, in the other configuration of sand, the Temisca 20 sand being on the upper part of the sandbox, the zone where bypass would occur could not be seen because the glass window did not cover the whole surface of sand filling. The contact of foam with the water present in the sandbox at the beginning of foam injection seems to make the foam unstable and separate it in liquid surfactant and slugs of air. The presence of liquid surfactant is clear in Figure 4.14 (d) where the black ellipse highlights a zone where the colored original water with tracer is diluted by liquid surfactant coming from the foam. This could imply that a loss of pressure is occurring because of the slugs of air that exit the sandbox before the foam front attains the outlet.

A glass window on the entire thickness of sand in the sandbox could be an improvement that would at least allow a visual assessment of bypasses. It implies that the entire tested zone could be seen, therefore indicating if any accumulation of contaminant or air occurred in the sandbox upper part. Also, it could allow a simplification of results interpretation since observations and photos of the sandbox would be more representative of the whole experiment.

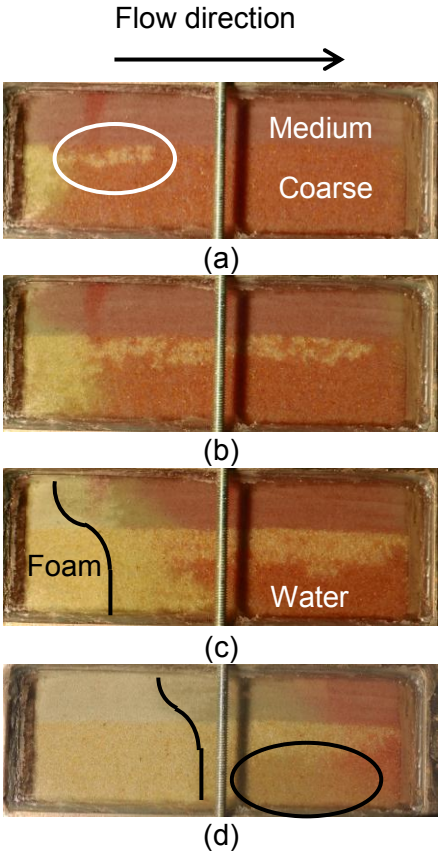

Figure 4.14 – Photos of foam injection in inverted configuration sandbox (coarser layer under finer layer), the black line indicates the foam front locations after (a) 7 sec, (b) 46 sec, (c) 4 min and (d) 1 hour after the start of injection in a non-contaminated sandbox.

4.5 Conclusions

Foam injection has many potential advantages that make it a promising LNAPL remediation technology: lowering of interfacial tension with the presence of surfactant for enhanced mobilization, mobility control achieved by an increase in viscosity and the use of air that can lower surfactant mass used, and cost, when compared with surfactant solution injection alone. This study aimed to better understand foam behavior in a context of layered soil contaminated with LNAPL. 2D sandbox tests were carried out in order to evaluate p-xylene recovery with Ammonyx Lo 0.1% in a porous media made up of two layers of silica sand with two different grain sizes and permeabilities.

Water injection with tracers indicated that contamination caused an increase in permeability ratio between both layers, which implies that contamination of the sandbox had a distinct effect on the two sand layers. Contamination reduced permeability in the medium sand layer more than in the coarse sand layer. Therefore, a good mobility control during treatment was even

more important in order to uniformly sweep the entire sandbox. Contrary to liquid tracer injection that had a piston shape and large gap between sand layers, uncontaminated foam test showed a foam front with an “S” shape in both sand layers where the front was advancing at the same velocity. The permeability contrast between sand layers was therefore compensated by the capacity of foam to create a front with good mobility control. Liquid surfactant injection in the contaminated sandbox did not perform well, even if the capillary number of 3.42×10^{-5} was theortically enough to mobilize some of the p-xylene residual saturation but not enough to entirely clean the sandbox. Foam injection in the contaminated sandbox, however, was efficient to clean both layers of the sandbox while advancing in an “S” shape front similar to what was observed during the uncontaminated foam test. Mobilization, volatilization and dissolution took place during foam treatment of the contaminated sandbox. However, a large uncertainty was related to the evaluation of volatilization because of difficulties in the evaluation of air flow rate. So, the total of mass recovered by all mechanisms only represents 48% of the initial p-xylene mass in the sandbox. This is not coherent with sand samples at the end of the test, which indicated a remaining mass of only 0.263 g (0.29% of initial contamination). Assuming that the missing mass was related to volatilization, it was possible to assess the proportions of recovery mechanisms: volatilization would then be responsible for 65% of the total recovery whereas mobilization and dissolution would be responsible for 19% and 16% respectively. A more precise air flow measurement system would be necessary for further testing. These results show how efficient foam injection can be for the treatment of p-xylene in heterogeneous porous media. This technology needs more research before a field application. Other sand box tests are suggested with foam generated in situ and with an injection and pumping system that use density contrasts to mobilise NAPL vertically and horizontally.

4.6 Acknowledgements

Funding of this study was provided by a NSERC-CRD grant in partnership with TechnoRem Inc and a NSERC-discovery grant of Richard Martel. The authors would like to gratefully acknowledge the help of Luc Trépanier and Guillaume Lefrançois in conceiving the experimental setup, Uta Gabriel for her advices during sandbox contamination and Richard Lévesque for sample analyses.

CHAPITRE 5 : CONCLUSIONS GÉNÉRALES ET RECOMMANDATIONS

L'objectif général de cette étude était de développer une méthodologie pour la sélection d'un tensioactif utilisé pour la production de mousse dans le but de traiter une contamination au LIL dans des sédiments peu profonds. Pour se faire, un ensemble de solutions tensioactives a été testé pour en définir les propriétés moussantes grâce au test Ross Miles et pour leur tension interfaciale avec le p-xylène grâce au test de la goutte pendante. Des essais en colonne ont ensuite été faits avec les solutions tensioactives sélectionnées afin de déterminer les conditions d'injection idéales dans un milieu homogène 1D. Puis, des essais ont été effectués afin d'évaluer les conditions d'écoulement de liquides et de mousses dans un bac 2D constitué de deux sables de granulométries différentes. Finalement, le bac 2D a été contaminé puis traité avec une solution tensioactive puis avec de la mousse.

Le test Ross Miles s'est montré efficace afin d'identifier les tensioactifs ayant de bonnes capacités moussantes. Les essais en colonne ont démontré que les solutions ayant présenté de meilleurs résultats lors du test Ross Miles ont aussi produit une mousse plus visqueuse et un front plus stable lors de l'injection en colonne. Le test Ross Miles étant simple et rapide à effectuer, il est donc un outil intéressant afin de classer les solutions tensioactives selon leur capacité à produire de la mousse. Les autres essais en colonne ont permis d'identifier certaines conditions à respecter en vue des essais en bac 2D. Afin d'obtenir un front de mousse stable et visqueux, les conditions suivantes sont nécessaires : une pression d'injection élevée, l'utilisation d'une colonne de production de mousse et la saturation de la colonne avec la solution tensioactive avant l'injection de la mousse.

Des essais en bac 2D ont été effectués en vue de tester le traitement avec de la mousse d'un sol hétérogène contaminé au p-xylène. Le bac était constitué de deux couches superposées de sables homogènes de granulométries différentes; un sable moyen surmonté d'un sable grossier. Les essais de traçage en conditions contaminées et non contaminées ont permis d'évaluer le contraste de perméabilité entre les deux couches de sable. Les résultats de ces essais ont mis en évidence un contraste plus marqué lorsque le bac était contaminé que lorsqu'il était seulement saturé en eau. La contamination du bac a diminué davantage la perméabilité du sable moyen que celle du sable grossier. Le contrôle de mobilité est alors devenu primordial afin d'obtenir un balayage efficace et complet des deux couches de sable. L'essai d'injection de mousse dans le bac non contaminé a permis d'observer un front stable en

forme de « S » avançant à la même vitesse dans les deux couches, indiquant un meilleur contrôle de mobilité que lors de l'injection du traceur qui avait créé un front en forme de piston qui avançait plus rapidement dans le sable grossier que dans le sable moyen.

Étant donné les résultats obtenus lors des essais d'injection de mousse en colonne, une saturation en solution tensioactive a été effectuée avant l'injection de mousse. Elle a été interprétée comme une méthode de traitement pour fins de comparaisons avec l'essai de traitement. Un nombre capillaire de 3.42×10^{-5} a été évalué pour l'essai ce qui a été suffisant pour amorcer la mobilisation de p-xylène mais pas pour le récupérer. L'injection de mousse a été efficace permettant que 99.71% du p-xylène initial soit retiré du bac de sable. Cependant, le bilan de masse indique que 51% de la masse a été récupérée par mobilisation, solubilisation et volatilisation. La différence entre les deux proportions de récupération est possiblement due à une évaluation erronée du volume d'air ayant traversé le bac. Considérant que la masse manquante soit reliée à la volatilisation, il a été possible de déterminer les proportions de recuperation de chaque mécanisme: la volatilisation serait responsible de 65% de la recuperation totale alors que la mobilisation et la solubilisation seraient responsables de 19% et 16% respectivement. Il serait donc nécessaire, pour des essais futurs, d'utiliser une méthode plus précise de mesure du débit d'air. Aussi, des pressions d'injection de mousse au-dessus de 500 cm d'eau ont été nécessaires pour que le front poursuive son avancée dans le bac contaminé. Dans l'optique d'une mise à l'échelle de la technologie pour une injection dans un aquifère non confiné peu profond, ces valeurs de pression sont trop élevées. Il faudrait donc trouver des options d'injection de mousse à plus faible pression.

CHAPITRE 6 : RÉFÉRENCES

Bear, J., 1972: Dynamics of fluids in porous media. Dover Publications, Inc., New York, 764 p.

Chowdiah, P., Misra, B.R, Kilbane, J.J., Srivastava, V.J., Hayes, T.D., 1998. Foam propagation through soils for enhanced in-situ remediation. J. Hazard. Mater., 62, 265– 280.

Couto, H.J.B., Massarani, G., Biscaia, E.C., Sant'Anna, G.L., 2009. Remediation of sandy soils using surfactant solutions and foams. Journal of Hazardous Materials, 164, 1325–1334.

Falls, A.H., Musters, J.J., and Ratulowski, J., 1989. The apparent viscosity of foams in homogeneous bead packs. SPE Reservoir Engineering, 155-164.

Farajzadeh, R., Andrianov, A., Hirasaki, G.J., Krastev, R., Rossen, W.R., 2012. Foam–oil interaction in porous media: implications for foam assisted enhanced oil recovery, Adv. Colloid Interface Sci., 183, 1–13.

Freeze, R.A., Cherry, J.A., 1979. Groundwater: Englewood Cliffs, NJ, Prentice-Hall, 604 p.

Hébert, J., Bernard, J., 2013. Bilan sur la gestion des terrains contaminés au 31 décembre 2010, ISBN 978-2-550-67511-2, 31 p.

Hirasaki, G.J., 1989. The steam-foam process. J. Pet. Technol., 41 (5), 449-456.

Hirasaki, G.J., Jackson, RE., Jin, M., Lawson, J.B., Londergan, J., Meinardus, H., Miller, C.A. et al*.,* 2000. "Field Demonstration of the Surfactant Foam Process for Remediation of a Heterogeneous Aquifer Contaminated with DNAPL," In *NAPL Removal: Surfactants, Foams, and Microemulsions*, ed. S. Fiorenza, C.A. Miller, C.L. Oubre, and C.H. Ward, Part 1, 3-163. AATDF monograph series, Boca Raton, Florida, USA: Lewis Publishers, CRC Press.

Hirasaki, G.J., Lawson, J.B., 1985. Mechanism of foam flow in porous media: apparent viscosity in smooth capillaries. SPEJ, 25 (2), 176–190.

Jeong, S.W., Corapcioglu, M.Y., Roosevelt, S.E., 2000. Micromodel study of surfactant foam remediation of residual trichloroethylene. Environ. Sci. Technol., 34, 3456-3461.

Jeong, S.W., Corapcioglu, M.Y., 2003. A micromodel analysis of factors influencing NAPL removal by surfactant foam flooding. Journal of Contaminant Hydrology, 60, 77–96.

Jeong, S.W., Corapcioglu, M.Y., 2005. Force analysis and visualization of NAPL removal during surfactant-related floods in a porous medium. Journal of Hazardous Materials, A126, 8–13

Johnson, P.C., Stanley, C.C., Kemblowski, M.W.,Byers, D.L., Colthart, J.D., 1990. A practical approach to the design, operation, and monitoring of in situ soil-venting systems. Groundwater Monitoring & Remediation, 10(2), 158-178.

Kovscek, A.R. and Radke, C.J., 1994. "Fundamentals of Foam Transport in Porous Media." In *Foams, Fundamentals and Applications in the Petroleum Industry*, ed. Schramm, L.L., ACS, Washington, DC.

Lake, L.W., 1989. Enhanced Oil Recovery. Prentice-Hall, Englewood Cliffs, NJ. 550 pp.

Li, R.F., 2011. Study of Foam Mobility Control in Surfactant Enhanced Oil Recovery Processes in 1-D, Heterogeneous 2-D, and Micro Model Systems. PhD Thesis, Rice University, Houston, Texas.

Li, R.F., Hirasaki, G.J., Miller, C.A., Masalmeh, S.K., 2012a. Wettability alteration and foam mobility Control in a layered, 2D heterogeneous sandpack, SPEJ, 17 (4), 1207-1220.

Li, X., Kaeakshev, S.I., Evans, G.M., Stevenson, P., 2012b. Effect of environmental humidity on static foam stability. Langmuir, 28, 4060−4068.

Manlowe, D.J., Radke, C.J., 1990. A pore-level investigation of foam/oil interactions in porous media. SPE Res. Eng., 5, 405–502.

Marsily, G. de, 1986. Quantitative hydrogeology - Groundwater hydrology for engineers. Academic Press Inc., San Diego, CA.

Martel, K.E., 1995. Utilisation de solutions de polymères pour améliorer l'efficacité de balayage des solutions tensioactives développées pour la restauration d'aquifères contaminés aux hydrocarbures immiscibles lourds. Thèse M.Sc., Département de géologie et génie géologique, Université Laval, Québec, Canada, 119 p.

Martel, K.E., Martel, R., Lefebvre, R., Gélinas, P., 1998. Laboratory study of polymer solutions used for mobility control during *in situ* NAPL recovery. *Ground Water Monitoring and Remediation*, 18(3), 103-113.

Martel, R., Hébert, A.R., Lefebvre, R., Gélinas, P.J., Gabriel, U., 2004. Displacement and sweep efficiencies in a DNAPL recovery test using micellar and polymer solutions injected in a five-spot pattern. Journal of Contaminant Hydrology, 75, 1–29.

Martel, T., Gélinas, P.J., 1996. Surfactant solutions developed for NAPL recovery in contaminated aquifers, Groundwater, 34, 143-154.

Ministère de l'Environnement du Québec (MEQ), 1998 et mises à jours subséquentes. Politique de protection des sols et de réhabilitation des terrains contaminés. Direction des politiques du secteur industriel – service des lieux contaminés. Les Publications du Québec, Sainte-Foy. 124p.

Mercer, J.W., Cohen, R.M., 1990. A review of immiscible fluids in the subsurface: properties, models, characterization and remediation. Journal of Contaminant Hydrology, 6, 107-163.

Mouton, J., Mercier, G., & Blais, J. F., 2009. Amphoteric surfactants for PAH and lead polluted-soil treatment using flotation. Water, Air, and Soil Pollution, 197, 381–393.

Mulligan, C.N., Eftekhari, F., 2003. Remediation with surfactant foam of PCP-contaminated soil. Engineering Geology, 70, 269–279.

Mulligan, C.N., Yong, R.N., Gibbs, B.F., 2001a. Surfactant-enhanced remediation of contaminated soil: a review. Eng. Geol., 60, 371–380.

Nguyen, Q.P., Currie, P.K., Buijse, M., Zitha, P.L.J., 2007. Mapping of foam mobility in porous media. Journal of Petroleum Science and Engineering, 58, 119–132.

Ogata, A., 1970. Theory of dispersion in a granular medium. U.S. Geological Survey Professional Paper 411-I, p.134.

Pennell, K.D., Pope, G.A., Abriola, L.W., 1996. Influence of viscous and buoyancy forces on the mobilization of residual tetrachloroethylene during surfactant flooding. Environmental Science and Technology, 30 (4), 1328-1335.

Ripple, C.D., James, R.V., Rubin, J., 1973. Radial particle-size segregation during packing of particle into cylindrical containers. Power Tech., 8, 165-175.

Robert, T., Martel, R., Conrad, S.H., Lefebvre, R., Gabriel, U., 2006. Visualization of TCE recovery mechanisms using surfactant-polymer in a two dimensional heterogeneous sand model. Journal of Contaminant Hydrology, 86, 3-31.

Rothmel, R.K., Peters, R.W., St. Martin, E., Deflaun, M.F., 1998. Surfactant foam biodegradation of in situ treatment of TCE DNAPLs. Environ. Sci. Technol., 32, 1667-1675.

Schramm, L.L., 2005. Emulsions, Foams, and Suspensions: Fundamentals and Applications, Wiley-VCH: Weinheim.

Shalcross, D.C., Castanier, L.M., Brigham, W.E., 1990. Characterization of steam foam surfactants through one-dimensional sandpack experiments. Stanford University Petroleum Research Institute, Stanford, California.

Silva, J.A.K., Smith, M.M., Munakata-Marr, J., McCray, J.E., 2012. The effect of system variables on in situ sweep-efficiency improvements via viscosity modification. Journal of Contaminant Hydrology, 136–137, 117–130.

Simjoo, M., Nguyen, Q.P., Zitha, P.L.J., 2012. Rheological Transition during Foam Flow in Porous Media. Ind. Eng. Chem. Res., 51, 10225−10231.

Simjoo, M., Dong, Y., Andrianov, A., Talanana, M., Zitha, P.L.J., 2013. CT scan study of immiscible foam flow in porous media for enhancing oil recovery. Ind. Eng.Chem. Res., 52, 6221–6233.

Tanzil, D., Hirasaki, G.J., and Miller, C.A., 2002a. Conditions for Foam Generation In Homogeneous Porous Media. SPE 75176.

Woodward, R.P., 2011. Surface Tension Measurements Using the Drop Shape Method. First Ten Angstroms. 6 p.